

Capturing Shock Waves by Relaxation Neural Networks

Nan Zhou¹ and Zheng Ma^{1, 2, 3, *}

¹School of Mathematical Sciences, Shanghai Jiao Tong University, Shanghai, 200240, China

²Institute of Natural Sciences, MOE-LSC, Shanghai Jiao Tong University, Shanghai, 200240, China

³CMA-Shanghai, Shanghai Jiao Tong University, Shanghai, 200240, China

April 2, 2024

Abstract

In this paper, we put forward a neural network framework to solve the nonlinear hyperbolic systems. This framework, named relaxation neural networks(RelaxNN), is a simple and scalable extension of physics-informed neural networks(PINN). It is shown later that a typical PINN framework struggles to handle shock waves that arise in hyperbolic systems' solutions. This ultimately results in the failure of optimization that is based on gradient descent in the training process. Relaxation systems provide a smooth asymptotic to the discontinuity solution, under the expectation that macroscopic problems can be solved from a microscopic perspective. Based on relaxation systems, the RelaxNN framework alleviates the conflict of losses in the training process of the PINN framework. In addition to the remarkable results demonstrated in numerical simulations, most of the acceleration techniques and improvement strategies aimed at the standard PINN framework can also be applied to the RelaxNN framework.

1 Introduction

Hyperbolic systems model a series of phenomena that involve wave motion and advective transport of substances. As the preferred mode for communicating information, they arise in the fields of gas dynamics, acoustics, optics, and so on. As for linear hyperbolic systems, the structure of the solution is perspicuous by decomposing any initial value problem into a Riemann problem through characteristic vectors. However, nonlinear hyperbolic systems frequently occur in a broad spectrum of disciplines. The nonlinearity, possibly leading to the formulation of shock waves, brings tremendous difficulties to solving the systems. Finite volume methods(FVM) are oriented to solve the nonlinear hyperbolic systems. Precisely, Godunov [1] proposed a general case of reconstruct-evolve-average(REA) algorithm for solving the nonlinear Euler equations. Based on the REA algorithm, a variety of high-resolution methods are designed for capturing shock waves nowadays such as essentially nonoscillatory(ENO) methods raised by Harten et al. [2], weighted ENO(WENO) methods

*Corresponding author: zhengma@sjtu.edu.cn

raised by Jiang and Shu [3]. Besides FVM, finite element methods(FEM) can also apply to non-linear hyperbolic systems through the discontinuous Galerkin method(DG) proposed by Cockburn et al. [4].

Rather than directly being faced with hyperbolic systems, we can approximate the solution of hyperbolic systems smoothly by modifying the hyperbolic systems. VonNeumann and Richtmyer [5] firstly capturing shock waves by introducing an artificial viscosity. However, adding viscous terms is intrinsically non-physical and is computationally expensive. Another way to obtain smooth asymptotics is to interpret the hydrodynamic equations from the microscopic perspective. In spirit to that, Jin [6] put forward a series of asymptotic preserving schemes for multiscale kinetic and hyperbolic equations.

Nowadays, the outstanding performance of deep learning attracts people’s attention. The idea of approximating the solution of partial differential equations by neural networks can date back to Dissanayake and Phan-Thien [7]. The theoretical guarantee for a continuous solution is the universal approximation theorem proposed by Hornik et al. [8]. With the roaring computational power, the unexpected results obtained by Physics-informed neural networks(PINN) [9] polish this field again. Such a lucid framework, characterized by the combination of data-driven(e.g., initial conditions and boundary conditions) and physical constraint(e.g., the governing equations), spread widely and has been applied to many fields[10]. Additionally, by taking advantage of automatic differentiation[11], the PINN framework is a non-mesh method that sheds light on breaking the curse of dimensionality.

However, several possible failure modes in PINN have been fully explored[12, 13, 14]. Solving the nonlinear hyperbolic systems is a kind of widely reported failure mode due to the discontinuity brought by shock waves [15, 16]. Naturally, improvement can be raised by the experience of traditional numerical methods. Patel et al. [17] proposed the control volume PINN and introduced the TVD condition into the framework. De Ryck et al. [18] raised the weak PINN for capturing shock waves. Above that, Chaumet and Giesselmann [15] gave a more efficient weak PINN scheme and entropy admissibility conditions for the uniqueness of the solution. Liu et al. [19] came up with weighted equations PINN method. Besides, introducing artificial viscosity directly or implicitly is also adopted to solve this problem [9, 20, 21]. Some of them obtained impressive results.

However, these methods make progress at the expense of losing the most attractive properties of deep learning. Introducing numerical derivatives or adopting the prior information about shock location, are making this simple framework mesh-dependent. Also, without the automatic differentiation, our training costs are getting higher and higher. All we need is to capture the shock automatically without losing the simplicity. Based on the relaxation systems proposed by Jin and Xin [22], we put forward the relaxation neural networks(RelaxNN) framework aiming at developing the basic method for solving hydrodynamic equations under the microscopic perspective. Besides the remarkable results we obtained, RelaxNN is a mild and scalable modification of PINN, reserving the simplicity and generality of PINN at the best effort. This means that many sampling strategies and training strategies for PINN could also be incorporated into the RelaxNN framework to acquire more precise results.

Besides the deterministic situations, many uncertainties must be considered due to insufficient knowledge about problems. After all, the closures of some conservation laws are empirical, which inevitably contain some uncertainties. Uncertainty Quantification(UQ) is a field aiming at systematically quantifying the uncertainties that propagate within our models. Along the mindset of UQ, we here consider random uncertainties for high-fidelity simulations [23], which is notoriously tough for its high-dimensional properties. Fortunately, methods based on the PINN framework, known

as deep-learning-based methods, are born to solve high-dimensional partial differential equations [24, 25, 9, 26, 27, 28, 29].

The paper is organized as follows. We give a brief introduction about conservation laws and relaxation systems in Section 2, Section 3. Section 4 introduces the PINN and briefly analyzes the latent failure reason for solving nonlinear hyperbolic systems. In Section 5, we propose the RelaxNN and give some possible modifications in specific cases. Finally, we implement our RelaxNN framework and compare our results with the solution obtained by Clawpack Development Team [30] in Section 6. We also demonstrate the potential of our method to overcome the curse of dimensionality through the lens of solving the uncertainty quantification problems at the end of the Section 6.

2 The conservation laws and the shock wave

From the fluid dynamics perspective, the conservation laws can arise from physics principles. In this article, we consider the systems of conservation laws in one space variable

$$\partial_t \mathbf{u} + \partial_x \mathbf{F}(\mathbf{u}) = 0, (t, x) \in \mathbb{R}_+ \times \mathbb{R}, \mathbf{u} \in \mathbb{R}^n, \quad (1)$$

where $\mathbf{F}(\mathbf{u}) \in \mathbb{R}^n$ is a vector-valued function, usually called a flux function. As for linear hyperbolic systems, the solution can be easily obtained since it can be viewed as the linear combination of the right vectors at each point in space-time. Physically, it is a superposition of waves propagating at different velocities. When it comes to nonlinear hyperbolic systems, the problem becomes intangible. The shock wave will form at the position where characteristic lines intersect. At those points, the conservation laws (1) cannot hold in the classic sense[31]. Usually, we step back to the fundamental integral conservation laws (2) in this circumstance,

$$\frac{d}{dt} \int_{x_1}^{x_2} \mathbf{u}(x, t) dx = \mathbf{F}(\mathbf{u}(x_1, t)) - \mathbf{F}(\mathbf{u}(x_2, t)), \quad (2)$$

for any two points x_1 and x_2 in \mathbb{R} . Furthermore, we pursue the weak solution of conservation law (1) in this case. $\mathbf{u}(t, x)$ is the weak solution of conservation law (1) with initial condition $\mathbf{u}(0, x) = \mathbf{u}_0(x)$ if

$$\int_0^\infty \int_{-\infty}^\infty [\mathbf{u} \phi_t + \mathbf{F}(\mathbf{u}) \phi_x] dx dt = - \int_0^\infty \mathbf{u}(0, x) \phi(0, x) dx, \quad (3)$$

holds for all functions $\phi \in C_0^1$ (continuously differentiable with compact support). In this paper, we mainly consider nonlinear hyperbolic systems.

3 The relaxation systems and the relaxation schemes

For the unfeasible nonlinear hyperbolic systems, the basic idea of the relaxation systems is to use a local relaxation approximation. So for any system of conservation laws, we can construct a corresponding linear hyperbolic system with a stiff source term that approximates the original system with a small dissipative correction.

Precisely, for the systems of conservation law in one space variable (1), Jin and Xin [22] introduced the corresponding relaxation system as

$$\begin{cases} \frac{\partial}{\partial t} \mathbf{u} + \frac{\partial}{\partial x} \mathbf{v} = 0, \quad \mathbf{v} \in \mathbb{R}^n, \\ \frac{\partial}{\partial t} \mathbf{v} + A \frac{\partial}{\partial x} \mathbf{u} = -\frac{1}{\varepsilon} (\mathbf{v} - \mathbf{F}(\mathbf{u})), \quad \varepsilon > 0, \end{cases} \quad (4)$$

where

$$A = \text{Diag}\{a_1, a_2, \dots, a_n\}, \quad (5)$$

is a chosen positive diagonal matrix. For small ε , applying the Chapman-Enskog expansion[32] in (4), we can obtain the following approximation for \mathbf{u} as [33, 34]

$$\frac{\partial}{\partial t} \mathbf{u} + \frac{\partial}{\partial x} \mathbf{F}(\mathbf{u}) = \varepsilon \frac{\partial}{\partial x} \left((A - \mathbf{F}'(\mathbf{u})^2) \frac{\partial}{\partial x} \mathbf{u} \right), \quad (6)$$

where $\mathbf{F}'(\mathbf{u})^2$ is the Jacobian matrix of the flux function $\mathbf{F}(\cdot)$. Obviously, Equation (6) governs the first-order behavior of the relaxation system (4).

Taking appropriate numerical discretizations to the relaxation system (4), we will obtain the relaxing schemes to the original conservation law. The solution of relaxing schemes will accurately approximate the solution of the original equation (1) when ε is sufficiently small. The linear structure of the relaxation system benefits us in avoiding the time-consuming Riemann solvers, which is inevitable to the high-resolution methods for nonlinear hyperbolic systems. The last point we need to pay attention to is to use proper implicit time discretizations to overcome the stability constraints due to the stiffness of the systems.

4 Physics-informed neural networks and its failure

For Cauchy problem of the conservation laws (1) with the initial condition

$$\mathbf{u}(0, x) = \mathbf{u}_0(x). \quad (7)$$

The PINNs framework for solving this problem is to approximate $\mathbf{u}(t, x)$ using a deep neural network $\mathbf{u}_\theta^{\text{NN}}(t, x)$ parameterized by trainable variables θ , then train the network by the physics information (e.g., the governing equations) and the given data (e.g., initial conditions and boundary conditions).

The loss function for training the $\mathbf{u}_\theta^{\text{NN}}(t, x)$ is defined as

$$\mathcal{L}_{\text{PINN}} = \omega_{\text{PDE}} \mathcal{L}_{\text{PDE}} + \omega_{\text{IC}} \mathcal{L}_{\text{IC}}, \quad (8a)$$

$$\mathcal{L}_{\text{PDE}} = \frac{1}{|\mathcal{T}_r|} \sum_{\mathbf{x} \in \mathcal{T}_r} (\partial_t \mathbf{u}_\theta^{\text{NN}}(\mathbf{x}_i) + \partial_x \mathbf{F}(\mathbf{u}_\theta^{\text{NN}}(\mathbf{x}_i)))^2, \quad (8b)$$

$$\mathcal{L}_{\text{IC}} = \frac{1}{|\mathcal{T}_{ic}|} \sum_{\mathbf{x} \in \mathcal{T}_{ic}} (\mathbf{u}_\theta^{\text{NN}}(\mathbf{x}_i) - \mathbf{u}_0(\mathbf{x}_i))^2, \quad (8c)$$

$$(8d)$$

where $\mathcal{T}_r \subset \Omega$, $\mathcal{T}_{ic} \subset \partial\Omega$ are the sets of "residual points" and $\omega_{\text{PDE}}, \omega_{\text{IC}}$ are the loss weights.

However, minimizing the strong form PDE loss function (Monte-Carlo approximation of L^2 -norm) will not work for learning discontinuous solutions to hyperbolic conservation laws because the conservation laws (1) near shock hold in the weak sense. Chaumet and Giesselmann [15] presents some analytic computations to explain this failure for inviscid Burgers' equation. In practice, this improper loss function constraint manifests that the PDE loss stagnates at a high level, which finally leads to the failure of gradient descent (see Figure 1a for an illuminating example). Also, we can find that the absolute error concentrates on $x = 0$ where there is a shock formed (see Figure 1b). An intuitive improvement is to adopt the weak form PDE loss function, De Ryck et al. [18] present

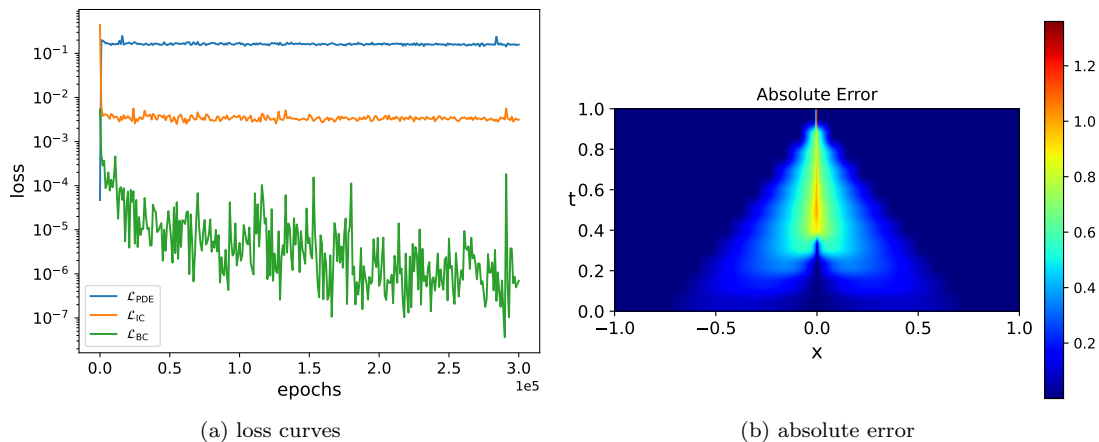


Figure 1: *Burgers' equation with Sine initial condition*: training a PINN model for approximating the solution to the Burgers' equation with sine initial condition : (a) loss curves along the training process. (b) absolute error between the prediction of PINN and the reference solution

the weak PINN for nonlinear hyperbolic systems and Chaumet and Giesselmann [15] come up with the more efficient weak PINN approximation based on the former work. Liu et al. [19] weaken the expression near shock to enhance the shock-capturing ability of PINN.

Another perspective is to obtain smooth asymptotics by modifying the hyperbolic systems (See Figure 2 for an overview diagram). With this mindset, adding artificial viscosity to dissipate oscillations is a common strategy. Whether directly solving the modified system with artificial viscosity [9, 20] or implicitly, replace the automatic differentiation with the numerical method in PDE loss [21]. But actually, it is a non-physical adjustment, which is inconsistent with the mindset of physics-informed deep learning. Based on the first principles in physics, the relaxation systems (4) is derived in spirit from the description of the hydrodynamic equations by the detailed microscopic evolution of gases in kinetic theory in the expectation that the complexity difficulties occurring at the macroscopic level can be illuminated by the hydrodynamic limit process.

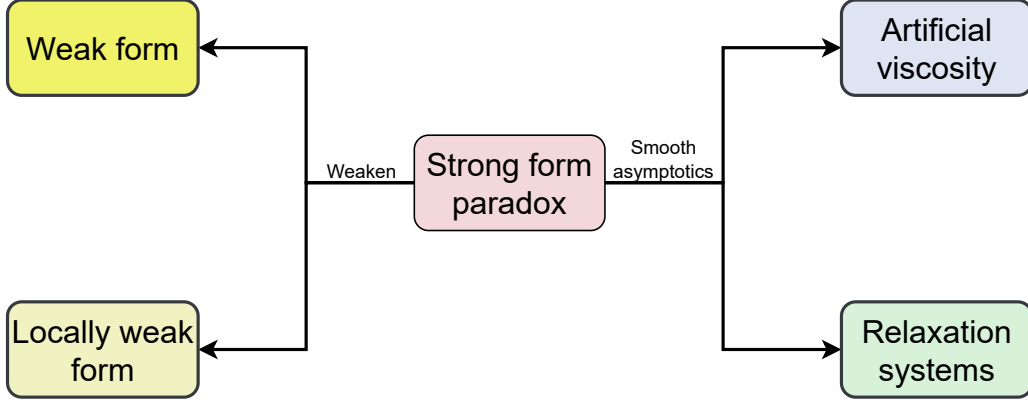


Figure 2: An overview diagram for different improvement ideas

5 Relaxation neural networks

For the Cauchy problem of the conservation laws (1) with the initial condition (7), the RelaxNN framework comprises two parts according to the relaxation systems (4), one approximates $\mathbf{u}(t, x)$ by a deep neural network $\mathbf{u}_{\theta_1}^{\text{NN}}(t, x)$ and another approximates \mathbf{v} by another deep neural network $\mathbf{v}_{\theta_2}^{\text{NN}}(t, x)$, separately parameterized by trainable variables θ_1 and θ_2 . If we solve the relaxation systems (4) with PINNs' framework, the PDE loss will be

$$\mathcal{L}_{\text{PDE}} = \mathcal{L}_{\text{residual}} + \mathcal{L}_{\text{dissipate}}, \quad (9a)$$

$$\mathcal{L}_{\text{residual}} = \frac{1}{|\mathcal{T}_r|} \sum_{\mathbf{x} \in \mathcal{T}_r} (\partial_t \mathbf{u}_{\theta_1}^{\text{NN}}(\mathbf{x}_i) + \partial_x \mathbf{v}_{\theta_2}^{\text{NN}}(\mathbf{x}_i))^2, \quad (9b)$$

$$\mathcal{L}_{\text{dissipate}} = \frac{1}{|\mathcal{T}_r|} \sum_{\mathbf{x} \in \mathcal{T}_r} (\varepsilon [\partial_t \mathbf{v}_{\theta_2}^{\text{NN}}(\mathbf{x}_i) + A \partial_x \mathbf{u}_{\theta_1}^{\text{NN}}(\mathbf{x}_i)] + \mathbf{v}_{\theta_2}^{\text{NN}}(\mathbf{x}_i) - \mathbf{F}(\mathbf{u}_{\theta_1}^{\text{NN}}(\mathbf{x}_i)))^2. \quad (9c)$$

In the small relaxation limit ($\varepsilon \rightarrow 0^+$),

$$\mathcal{L}_{\text{dissipate}} \approx \mathcal{L}_{\text{flux}} \triangleq \frac{1}{|\mathcal{T}_r|} \sum_{\mathbf{x} \in \mathcal{T}_r} (\mathbf{v}_{\theta_2}^{\text{NN}}(\mathbf{x}_i) - \mathbf{F}(\mathbf{u}_{\theta_1}^{\text{NN}}(\mathbf{x}_i)))^2. \quad (10)$$

In fact, the RelaxNN framework for the original conservation laws (1) is the PINN framework to the following modified relaxation systems (See Figure 3 for the relationship of different systems)

$$\begin{cases} \frac{\partial}{\partial t} \mathbf{u} + \frac{\partial}{\partial x} \mathbf{v} = 0, & \mathbf{u}, \mathbf{v} \in \mathbb{R}^n, \\ \mathbf{v} - \mathbf{F}(\mathbf{u}) = 0. \end{cases} \quad (11)$$

In traditional numerical methods, for the relaxation system (4), we must choose the initial condition as

$$\mathbf{u}(0, x) = \mathbf{u}_0(0, x), \quad (12a)$$

$$\mathbf{v}(0, x) = \mathbf{v}_0(0, x) \triangleq \mathbf{F}(\mathbf{u}_0(0, x)). \quad (12b)$$

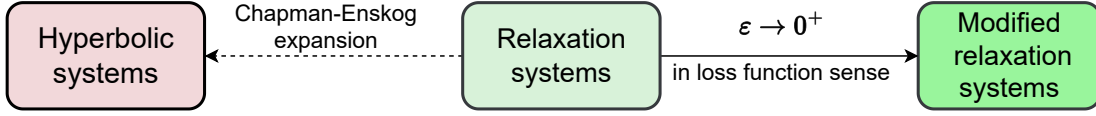


Figure 3: Brief illustration about the relationship of different systems mentioned above. Here the dashed line represents the low-order approximation.

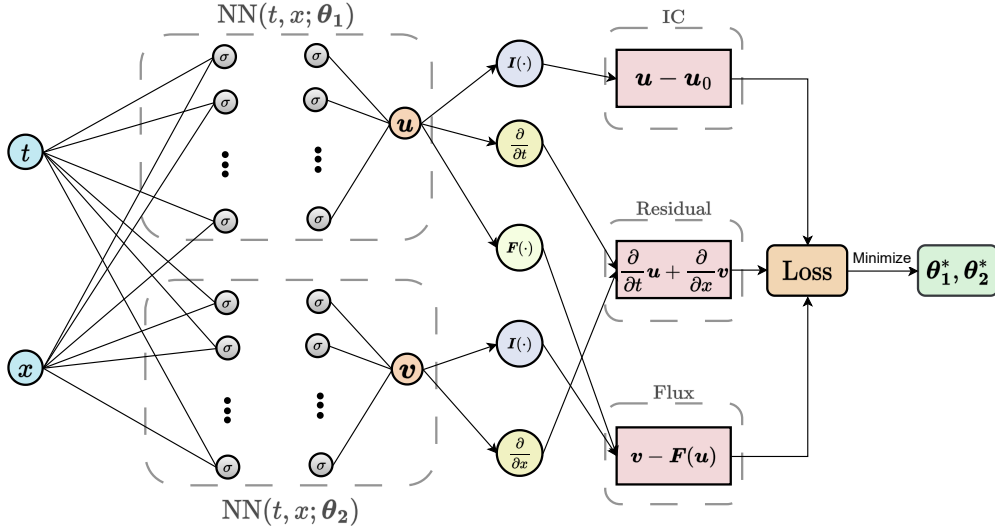


Figure 4: The schematic diagram of the RelaxNN to solve the hyperbolic systems with initial condition (IC) \mathbf{u}_0 and flux function $\mathbf{F}(\cdot)$.

Choosing the special initial condition for \mathbf{v} is to avoid the introduction of an initial layer through the relaxation system because of its stiffness. Now we do not need to impose the special initial condition penalty for the neural network $\mathbf{v}_{\theta_2}^{\text{NN}}(t, x)$ since we replace the $\mathcal{L}_{\text{dissipate}}$ with $\mathcal{L}_{\text{flux}}$ during the optimization process. So the training loss for the relaxation neural networks will be defined as

$$\mathcal{L}_{\text{RelaxNN}} = \omega_{\text{residual}} \mathcal{L}_{\text{residual}} + \omega_{\text{flux}} \mathcal{L}_{\text{flux}} + \omega_{\text{IC}} \mathcal{L}_{\text{IC}}. \quad (13)$$

See the visualization of RelaxNN in Figure 4.

Sometimes, we do not need to relax the whole hyperbolic system. The relaxation system is still linear if we only relax some of the conservation laws (e.g., the conservation law of momentum or energy). Additionally, the numerical methods for the original relaxation system are not always well-balanced and thus introduce spurious waves [35]. Similar to Suliciu's relaxation and its applications [36, 37, 38], Liu et al. [35] introduce the partial relaxation system which only relaxes the second equation of the Saint-Venant system of shallow water equations. In this article, we adopt and generalize the partial relaxation systems. Later we will make a more precise illustration of the specified equations we are concerned with.

5.1 Inviscid Burgers' equation

We first consider the inviscid Burgers' equation, the simplest hyperbolic equation with shock wave

$$\partial_t u + \partial_x \left(\frac{1}{2} u^2 \right) = 0. \quad (14)$$

The modified relaxation systems for Burgers' equation are

$$\begin{cases} \frac{\partial}{\partial t} u + \frac{\partial}{\partial x} v = 0, \\ v - \frac{1}{2} u^2 = 0. \end{cases} \quad (15)$$

For brevity, denote $\mathbf{u}_{\theta_1}^{\text{NN}} = u_{\theta_1}^{\text{NN}}$ approximates u and $\mathbf{v}_{\theta_2}^{\text{NN}} = v_{\theta_2}^{\text{NN}}$ approximates v , the residual loss term and flux loss term of RelaxNN framework can be presented more precisely as

$$\mathcal{L}_{\text{residual}} = \frac{1}{|\mathcal{T}_r|} \sum_{\mathbf{x} \in \mathcal{T}_r} \left(\partial_t u_{\theta_1}^{\text{NN}}(\mathbf{x}_i) + \partial_x v_{\theta_2}^{\text{NN}}(\mathbf{x}_i) \right)^2, \quad (16a)$$

$$\mathcal{L}_{\text{flux}} = \frac{1}{|\mathcal{T}_r|} \sum_{\mathbf{x} \in \mathcal{T}_r} \left(v_{\theta_2}^{\text{NN}}(\mathbf{x}_i) - \frac{1}{2} (u_{\theta_1}^{\text{NN}}(\mathbf{x}_i))^2 \right)^2. \quad (16b)$$

5.2 Shallow water equations

The shallow water equations describe the evolution of the incompressible fluid (constant density) with small-amplitude waves on the surface of the sphere

$$\begin{cases} \partial_t h + \partial_x (hu) = 0, \\ \partial_t (hu) + \partial_x \left(hu^2 + \frac{1}{2} gh^2 \right) = 0, \end{cases} \quad (17)$$

here h is the depth, u is the velocity and g is the gravitational constant.

5.2.1 Type1 fully modified relaxation systems

Here we can relax the whole hyperbolic system with the type1 fully modified relaxation systems as

$$\begin{cases} \frac{\partial}{\partial t} h + \frac{\partial}{\partial x} v = 0, \\ \frac{\partial}{\partial t} (hu) + \frac{\partial}{\partial x} \varphi = 0, \\ v - hu = 0, \\ \varphi - (hu^2 + \frac{1}{2} gh^2) = 0. \end{cases} \quad (18)$$

Denote $\mathbf{u}_{\theta_1}^{\text{NN}} = (h_{\theta_1}^{\text{NN}}, u_{\theta_1}^{\text{NN}})^{\text{T}}$ approximates $(h, u)^{\text{T}}$ and $\mathbf{v}_{\theta_2}^{\text{NN}} = (v_{\theta_2}^{\text{NN}}, \varphi_{\theta_2}^{\text{NN}})^{\text{T}}$ approximates $(v, \varphi)^{\text{T}}$, the loss function of RelaxNN framework can be presented as

$$\mathcal{L}_{\text{RelaxNN}}^{\text{type1}} = \omega_{\text{residual}} \mathcal{L}_{\text{residual}}^{\text{type1}} + \omega_{\text{flux}} \mathcal{L}_{\text{flux}}^{\text{type1}} + \omega_{\text{IC}} \mathcal{L}_{\text{IC}}, \quad (19)$$

where the residual loss term can be presented as

$$\begin{aligned}\mathcal{L}_{\text{residual}}^{\text{type1}} &= \frac{\omega_r^m}{|\mathcal{T}_r|} \sum_{\mathbf{x} \in \mathcal{T}_r} (\partial_t h_{\boldsymbol{\theta}_1}^{\text{NN}}(\mathbf{x}_i) + \partial_x v_{\boldsymbol{\theta}_2}^{\text{NN}}(\mathbf{x}_i))^2 \\ &+ \frac{\omega_r^p}{|\mathcal{T}_r|} \sum_{\mathbf{x} \in \mathcal{T}_r} (\partial_t (h_{\boldsymbol{\theta}_1}^{\text{NN}} u_{\boldsymbol{\theta}_1}^{\text{NN}})(\mathbf{x}_i) + \partial_x \varphi_{\boldsymbol{\theta}_2}^{\text{NN}}(\mathbf{x}_i))^2,\end{aligned}\quad (20)$$

and the flux loss term can be presented as

$$\begin{aligned}\mathcal{L}_{\text{flux}}^{\text{type1}} &= \frac{\omega_f^m}{|\mathcal{T}_r|} \sum_{\mathbf{x} \in \mathcal{T}_r} (v_{\boldsymbol{\theta}_2}^{\text{NN}}(\mathbf{x}_i) - (h_{\boldsymbol{\theta}_1}^{\text{NN}} u_{\boldsymbol{\theta}_1}^{\text{NN}})(\mathbf{x}_i))^2 \\ &+ \frac{\omega_f^p}{|\mathcal{T}_r|} \sum_{\mathbf{x} \in \mathcal{T}_r} \left(\varphi_{\boldsymbol{\theta}_2}^{\text{NN}}(\mathbf{x}_i) - \left(h_{\boldsymbol{\theta}_1}^{\text{NN}} (u_{\boldsymbol{\theta}_1}^{\text{NN}})^2 + \frac{1}{2} g (h_{\boldsymbol{\theta}_1}^{\text{NN}})^2 \right) (\mathbf{x}_i) \right)^2.\end{aligned}\quad (21)$$

5.2.2 Type2 partially modified relaxation systems

However, we can also only relax the conservation law of momentum with the type2 partial relaxation systems as

$$\begin{cases} \frac{\partial}{\partial t} h + \frac{\partial}{\partial x} (hu) = 0, \\ \frac{\partial}{\partial t} (hu) + \frac{\partial}{\partial x} \varphi = 0, \\ \varphi - (hu^2 + \frac{1}{2} gh^2) = 0. \end{cases}\quad (22)$$

Denote $\mathbf{u}_{\boldsymbol{\theta}_1}^{\text{NN}} = (h_{\boldsymbol{\theta}_1}^{\text{NN}}, u_{\boldsymbol{\theta}_1}^{\text{NN}})^{\text{T}}$ approximates $(h, u)^{\text{T}}$ and $\mathbf{v}_{\boldsymbol{\theta}_2}^{\text{NN}} = \varphi_{\boldsymbol{\theta}_2}^{\text{NN}}$ approximates φ , the loss function of RelaxNN framework can be presented as

$$\mathcal{L}_{\text{RelaxNN}}^{\text{type2}} = \omega_{\text{residual}} \mathcal{L}_{\text{residual}}^{\text{type2}} + \omega_{\text{flux}} \mathcal{L}_{\text{flux}}^{\text{type2}} + \omega_{\text{IC}} \mathcal{L}_{\text{IC}},\quad (23)$$

where the residual loss term can be presented as

$$\begin{aligned}\mathcal{L}_{\text{residual}}^{\text{type2}} &= \frac{\omega_r^m}{|\mathcal{T}_r|} \sum_{\mathbf{x} \in \mathcal{T}_r} (\partial_t h_{\boldsymbol{\theta}_1}^{\text{NN}}(\mathbf{x}_i) + \partial_x (h_{\boldsymbol{\theta}_1}^{\text{NN}} u_{\boldsymbol{\theta}_1}^{\text{NN}})(\mathbf{x}_i))^2 \\ &+ \frac{\omega_r^p}{|\mathcal{T}_r|} \sum_{\mathbf{x} \in \mathcal{T}_r} (\partial_t (h_{\boldsymbol{\theta}_1}^{\text{NN}} u_{\boldsymbol{\theta}_1}^{\text{NN}})(\mathbf{x}_i) + \partial_x \varphi_{\boldsymbol{\theta}_2}^{\text{NN}}(\mathbf{x}_i))^2,\end{aligned}\quad (24)$$

and the flux loss term can be presented as

$$\mathcal{L}_{\text{flux}}^{\text{type2}} = \frac{\omega_f^p}{|\mathcal{T}_r|} \sum_{\mathbf{x} \in \mathcal{T}_r} \left(\varphi_{\boldsymbol{\theta}_2}^{\text{NN}}(\mathbf{x}_i) - \left(h_{\boldsymbol{\theta}_1}^{\text{NN}} (u_{\boldsymbol{\theta}_1}^{\text{NN}})^2 + \frac{1}{2} g (h_{\boldsymbol{\theta}_1}^{\text{NN}})^2 \right) (\mathbf{x}_i) \right)^2.\quad (25)$$

5.3 Euler equations

The Euler equations are the conservation laws governing the compressible, adiabatic, and inviscid flow in fluid dynamics. Here, we consider 1 – D Euler equations of gas dynamics in conservative

forms

$$\begin{cases} \partial_t \rho + \partial_x (\rho u) = 0, \\ \partial_t (\rho u) + \partial_x (\rho u^2 + p) = 0, \\ \partial_t E + \partial_x (u(E + p)) = 0, \end{cases} \quad (26)$$

here ρ is the density, u is the velocity and p is the pressure for an ideal gas. To close the system of equations, we introduce the equation of state for an ideal polytropic gas

$$E = \frac{p}{\gamma - 1} + \frac{1}{2} \rho u^2, \quad (27)$$

with $\gamma = 1.4$ for a diatomic gas.

5.3.1 Type1 fully modified relaxation systems

Here we can relax the whole hyperbolic systems with the type1 fully modified relaxation systems as

$$\begin{cases} \frac{\partial}{\partial t} \rho + \frac{\partial}{\partial x} v = 0, \\ \frac{\partial}{\partial t} (\rho u) + \frac{\partial}{\partial x} \varphi = 0, \\ \frac{\partial}{\partial t} (E) + \frac{\partial}{\partial x} \zeta = 0, \\ v - (\rho u) = 0, \\ \varphi - (\rho u^2 + p) = 0, \\ \zeta - (u(E + p)) = 0. \end{cases} \quad (28)$$

Denote $\mathbf{u}_{\theta_1}^{\text{NN}} = (\rho_{\theta_1}^{\text{NN}}, u_{\theta_1}^{\text{NN}}, p_{\theta_1}^{\text{NN}})^{\text{T}}$ approximates $(\rho, u, p)^{\text{T}}$ and $\mathbf{v}_{\theta_2}^{\text{NN}} = (v_{\theta_2}^{\text{NN}}, \varphi_{\theta_2}^{\text{NN}}, \zeta_{\theta_2}^{\text{NN}})^{\text{T}}$ approximates $(v, \varphi, \zeta)^{\text{T}}$, the loss function of RelaxNN framework can be presented as

$$\mathcal{L}_{\text{RelaxNN}}^{\text{type1}} = \omega_{\text{residual}} \mathcal{L}_{\text{residual}}^{\text{type1}} + \omega_{\text{flux}} \mathcal{L}_{\text{flux}}^{\text{type1}} + \omega_{\text{IC}} \mathcal{L}_{\text{IC}}, \quad (29)$$

where the residual loss term can be presented as

$$\begin{aligned} \mathcal{L}_{\text{residual}}^{\text{type1}} &= \frac{\omega_r^m}{|\mathcal{T}_r|} \sum_{\mathbf{x} \in \mathcal{T}_r} (\partial_t \rho_{\theta_1}^{\text{NN}}(\mathbf{x}_i) + \partial_x v_{\theta_2}^{\text{NN}}(\mathbf{x}_i))^2 \\ &+ \frac{\omega_r^p}{|\mathcal{T}_r|} \sum_{\mathbf{x} \in \mathcal{T}_r} (\partial_t (\rho_{\theta_1}^{\text{NN}} u_{\theta_1}^{\text{NN}})(\mathbf{x}_i) + \partial_x \varphi_{\theta_2}^{\text{NN}}(\mathbf{x}_i))^2 \\ &+ \frac{\omega_r^e}{|\mathcal{T}_r|} \sum_{\mathbf{x} \in \mathcal{T}_r} \left(\partial_t \left(\frac{1}{\gamma - 1} \rho_{\theta_1}^{\text{NN}} + \frac{1}{2} \rho_{\theta_1}^{\text{NN}} (u_{\theta_1}^{\text{NN}})^2 \right) (\mathbf{x}_i) + \partial_x \zeta_{\theta_2}^{\text{NN}}(\mathbf{x}_i) \right)^2, \end{aligned} \quad (30)$$

and the flux loss term can be presented as

$$\begin{aligned}
\mathcal{L}_{\text{flux}}^{\text{type1}} &= \frac{\omega_f^m}{|\mathcal{T}_r|} \sum_{\mathbf{x} \in \mathcal{T}_r} (v_{\theta_2}^{\text{NN}}(\mathbf{x}_i) - (\rho_{\theta_1}^{\text{NN}} u_{\theta_1}^{\text{NN}})(\mathbf{x}_i))^2 \\
&+ \frac{\omega_f^p}{|\mathcal{T}_r|} \sum_{\mathbf{x} \in \mathcal{T}_r} (\varphi_{\theta_2}^{\text{NN}}(\mathbf{x}_i) - (\rho_{\theta_1}^{\text{NN}} (u_{\theta_1}^{\text{NN}})^2 + p_{\theta_1}^{\text{NN}})(\mathbf{x}_i))^2 \\
&+ \frac{\omega_f^e}{|\mathcal{T}_r|} \sum_{\mathbf{x} \in \mathcal{T}_r} \left(\zeta_{\theta_2}^{\text{NN}}(\mathbf{x}_i) - \left(\frac{\gamma}{\gamma-1} \rho_{\theta_1}^{\text{NN}} u_{\theta_1}^{\text{NN}} + \frac{1}{2} \rho_{\theta_1}^{\text{NN}} (u_{\theta_1}^{\text{NN}})^3 \right) (\mathbf{x}_i) \right)^2.
\end{aligned} \tag{31}$$

5.3.2 Type2 partially modified relaxation systems

Also, we can relax the conservation laws of momentum and energy with the type2 partially modified relaxation systems as

$$\begin{cases} \frac{\partial}{\partial t} \rho + \frac{\partial}{\partial x} (\rho u) = 0, \\ \frac{\partial}{\partial t} (\rho u) + \frac{\partial}{\partial x} \varphi = 0, \\ \frac{\partial}{\partial t} (\text{E}) + \frac{\partial}{\partial x} \zeta = 0, \\ \varphi - (\rho u^2 + p) = 0, \\ \zeta - (u(\text{E} + p)) = 0. \end{cases} \tag{32}$$

Denote $\mathbf{u}_{\theta_1}^{\text{NN}} = (\rho_{\theta_1}^{\text{NN}}, u_{\theta_1}^{\text{NN}}, p_{\theta_1}^{\text{NN}})^{\text{T}}$ approximates $(\rho, u, p)^{\text{T}}$ and $\mathbf{v}_{\theta_2}^{\text{NN}} = (\varphi_{\theta_2}^{\text{NN}}, \zeta_{\theta_2}^{\text{NN}})^{\text{T}}$ approximates $(\varphi, \zeta)^{\text{T}}$, the loss function of RelaxNN framework can be presented as

$$\mathcal{L}_{\text{RelaxNN}}^{\text{type2}} = \omega_{\text{residual}} \mathcal{L}_{\text{residual}}^{\text{type2}} + \omega_{\text{flux}} \mathcal{L}_{\text{flux}}^{\text{type2}} + \omega_{\text{IC}} \mathcal{L}_{\text{IC}}, \tag{33}$$

where the residual loss term can be presented as

$$\begin{aligned}
\mathcal{L}_{\text{residual}}^{\text{type2}} &= \frac{\omega_r^m}{|\mathcal{T}_r|} \sum_{\mathbf{x} \in \mathcal{T}_r} (\partial_t \rho_{\theta_1}^{\text{NN}}(\mathbf{x}_i) + \partial_x (\rho_{\theta_1}^{\text{NN}} u_{\theta_1}^{\text{NN}})(\mathbf{x}_i))^2 \\
&+ \frac{\omega_r^p}{|\mathcal{T}_r|} \sum_{\mathbf{x} \in \mathcal{T}_r} (\partial_t (\rho_{\theta_1}^{\text{NN}} u_{\theta_1}^{\text{NN}})(\mathbf{x}_i) + \partial_x (\rho_{\theta_1}^{\text{NN}} (u_{\theta_1}^{\text{NN}})^2 + p_{\theta_1}^{\text{NN}})(\mathbf{x}_i))^2 \\
&+ \frac{\omega_r^e}{|\mathcal{T}_r|} \sum_{\mathbf{x} \in \mathcal{T}_r} \left(\partial_t \left(\frac{1}{\gamma-1} \rho_{\theta_1}^{\text{NN}} + \frac{1}{2} \rho_{\theta_1}^{\text{NN}} (u_{\theta_1}^{\text{NN}})^2 \right) (\mathbf{x}_i) + \partial_x \zeta_{\theta_2}^{\text{NN}}(\mathbf{x}_i) \right)^2,
\end{aligned} \tag{34}$$

and the flux loss term can be presented as

$$\begin{aligned}
\mathcal{L}_{\text{flux}}^{\text{type2}} &= \frac{\omega_f^p}{|\mathcal{T}_r|} \sum_{\mathbf{x} \in \mathcal{T}_r} (\varphi_{\theta_2}^{\text{NN}}(\mathbf{x}_i) - (\rho_{\theta_1}^{\text{NN}} (u_{\theta_1}^{\text{NN}})^2 + p_{\theta_1}^{\text{NN}})(\mathbf{x}_i))^2 \\
&+ \frac{\omega_f^e}{|\mathcal{T}_r|} \sum_{\mathbf{x} \in \mathcal{T}_r} \left(\zeta_{\theta_2}^{\text{NN}}(\mathbf{x}_i) - \left(\frac{\gamma}{\gamma-1} \rho_{\theta_1}^{\text{NN}} u_{\theta_1}^{\text{NN}} + \frac{1}{2} \rho_{\theta_1}^{\text{NN}} (u_{\theta_1}^{\text{NN}})^3 \right) (\mathbf{x}_i) \right)^2.
\end{aligned} \tag{35}$$

5.3.3 Type3 partially modified relaxation systems

Of course, we can only relax the conservation law of energy with the type3 partially modified relaxation systems as

$$\begin{cases} \frac{\partial}{\partial t}\rho + \frac{\partial}{\partial x}(\rho u) = 0, \\ \frac{\partial}{\partial t}(\rho u) + \frac{\partial}{\partial x}(\rho u^2 + p) = 0, \\ \frac{\partial}{\partial t}(E) + \frac{\partial}{\partial x}\zeta = 0, \\ \zeta - (u(E + p)) = 0. \end{cases} \quad (36)$$

Denote $\mathbf{u}_{\theta_1}^{\text{NN}} = (\rho_{\theta_1}^{\text{NN}}, u_{\theta_1}^{\text{NN}}, p_{\theta_1}^{\text{NN}})^{\text{T}}$ approximates $(\rho, u, p)^{\text{T}}$ and $\mathbf{v}_{\theta_2}^{\text{NN}} = \zeta_{\theta_2}^{\text{NN}}$ approximates ζ , the loss function of RelaxNN framework can be presented as

$$\mathcal{L}_{\text{RelaxNN}}^{\text{type3}} = \omega_{\text{residual}}\mathcal{L}_{\text{residual}}^{\text{type3}} + \omega_{\text{flux}}\mathcal{L}_{\text{flux}}^{\text{type3}} + \omega_{\text{IC}}\mathcal{L}_{\text{IC}}, \quad (37)$$

where the residual loss term can be presented as

$$\begin{aligned} \mathcal{L}_{\text{residual}}^{\text{type3}} &= \frac{\omega_r^m}{|\mathcal{T}_r|} \sum_{\mathbf{x} \in \mathcal{T}_r} (\partial_t \rho_{\theta_1}^{\text{NN}}(\mathbf{x}_i) + \partial_x(\rho_{\theta_1}^{\text{NN}} u_{\theta_1}^{\text{NN}}(\mathbf{x}_i)))^2 \\ &+ \frac{\omega_r^p}{|\mathcal{T}_r|} \sum_{\mathbf{x} \in \mathcal{T}_r} (\partial_t(\rho_{\theta_1}^{\text{NN}} u_{\theta_1}^{\text{NN}})(\mathbf{x}_i) + \partial_x(\rho_{\theta_1}^{\text{NN}}(u_{\theta_1}^{\text{NN}})^2 + p_{\theta_1}^{\text{NN}})(\mathbf{x}_i))^2 \\ &+ \frac{\omega_r^e}{|\mathcal{T}_r|} \sum_{\mathbf{x} \in \mathcal{T}_r} \left(\partial_t \left(\frac{1}{\gamma-1} \rho_{\theta_1}^{\text{NN}} + \frac{1}{2} \rho_{\theta_1}^{\text{NN}}(u_{\theta_1}^{\text{NN}})^2 \right) (\mathbf{x}_i) + \partial_x \zeta_{\theta_2}^{\text{NN}}(\mathbf{x}_i) \right)^2, \end{aligned} \quad (38)$$

and the flux loss term can be presented as

$$\mathcal{L}_{\text{flux}}^{\text{type3}} = \frac{\omega_f^e}{|\mathcal{T}_r|} \sum_{\mathbf{x} \in \mathcal{T}_r} \left(\zeta_{\theta_2}^{\text{NN}}(\mathbf{x}_i) - \left(\frac{\gamma}{\gamma-1} \rho_{\theta_1}^{\text{NN}} u_{\theta_1}^{\text{NN}} + \frac{1}{2} \rho_{\theta_1}^{\text{NN}}(u_{\theta_1}^{\text{NN}})^3 \right) (\mathbf{x}_i) \right)^2. \quad (39)$$

6 Numerical examples

To illustrate the effectiveness of RelaxNN, we conduct a series of experiments about capturing shock waves. For the systems of conservation laws with an initial condition in the finite domain :

$$\begin{cases} \partial_t \mathbf{u} + \partial_x \mathbf{F}(\mathbf{u}) = 0, & (t, x) \in \Omega, \\ \mathbf{u}(t, x) = \mathbf{u}_0(t, x), & (t, x) \in \partial\Omega, \end{cases} \quad (40)$$

we impose the boundary condition as the same as the initial condition on the assumption that waves do not propagate to the boundary in the finite period we considered. In this case, the loss function for PINN and RelaxNN will be :

$$\mathcal{L}_{\text{PINN}} = \omega_{\text{PDE}}\mathcal{L}_{\text{PDE}} + \omega_{\text{IC}}\mathcal{L}_{\text{IC}} + \omega_{\text{BC}}\mathcal{L}_{\text{BC}}, \quad (41a)$$

$$\mathcal{L}_{\text{RelaxNN}} = \omega_{\text{residual}}\mathcal{L}_{\text{residual}} + \omega_{\text{flux}}\mathcal{L}_{\text{flux}} + \omega_{\text{IC}}\mathcal{L}_{\text{IC}} + \omega_{\text{BC}}\mathcal{L}_{\text{BC}}. \quad (41b)$$

Examples	Relax level	$\mathbf{u}_{\theta_1}^{\text{NN}}$				$\mathbf{v}_{\theta_2}^{\text{NN}}$			
		d_{in}	N_{depth}	N_{width}	d_{out}	d_{in}	N_{depth}	N_{width}	d_{out}
Burgers' Equation			4	128	1		4	64	1
Shallow Water Equations	type1		5	128	2		5	128	2
	type2	2	5	128	2	2	5	64	1
	type1		6	384	3		6	384	3
Euler Equations	type2		6	384	3		6	256	2
	type3		6	384	3		6	128	1

Table 1: Networks' configuration for all examples. Here d_{in} , d_{out} , N_{depth} , N_{width} represent the input dimension, the output dimension, the depth and width of the hidden layers of the specified neural network. Here d_{out} of $\mathbf{v}_{\theta_2}^{\text{NN}}$ indicates that how many conservation laws we relaxed.

Here \mathcal{L}_{BC} is defined as same as \mathcal{L}_{IC} excepts $\mathbf{x} \in \mathcal{T}_{bc}$, $\mathcal{T}_{bc} \subset \partial\Omega$ are the residual points sampled on the boundary.

For all experiments, training points are sampled randomly in uniform distribution. For conciseness, we roughly set $|\mathcal{T}_r| = 2540$, $|\mathcal{T}_{ic}| = 320$ and $|\mathcal{T}_{bc}| = 160$ for all experiments. Also, we set the random seed to 1 for all packages to ensure repeatability. For the architecture of the neural network, we employ the fully connected deep neural networks (DNNs) with "tanh" activation functions and He uniform initialization [39] for all experiments. For the training settings, we adopt "Adam"[40] Optimizer with an initial learning rate $1e - 3$, decaying exponentially for every 1000 epochs with a decay rate 0.99 during the whole training process for all experiments. We compare our results with high-resolution numerical methods obtained by clawpack [30]. Besides the remarkable performance, the comparison among the several types of RelaxNN also confirms our hypothesis about the generation of spurious waves. Later, we will see that the mild oscillation occurs only on the type1 RelaxNN schemes for shallow water equations, as well as type1 and type2 RelaxNN schemes for Euler's equations although both RelaxNN schemes are able to capture the shock waves and acquire outstanding performance. This interesting phenomenon also embodies Occam's razor theorem.

6.1 Inviscid Burgers' equation

6.1.1 Riemann problem

We consider the inviscid Burgers' equation in domain $\Omega = \{(t, x)\} = [0.0, 1.0] \times [-0.6, 0.6]$ with Riemann initial condition as

$$u_0(0, x) = \begin{cases} 1.0, & -0.6 \leq x \leq 0 \\ 0.0, & 0 < x \leq 0.6 \end{cases}. \quad (42)$$

Networks' configurations are presented in Table 1 and weights settings are shown in Table 2. With these settings, we train RelaxNN for 300,000 epochs and one step for every epoch. For the PINN framework, settings are the same without the extra neural network $\mathbf{v}_{\theta_2}^{\text{NN}}$. In Figure 5a, We compare the total loss between the PINN and RelaxNN. In Figure 6, we compare the prediction of RelaxNN and PINN at the final epoch for some specific times.

Problems	Relax level	ω_{residual}	ω_{flux}	ω_{IC}	ω_{BC}
Riemann Problem		0.1	2.0	10	10
Sine Problem		0.5	2.0	5.0	5.0

Table 2: *Burgers' equation*: Loss weights settings

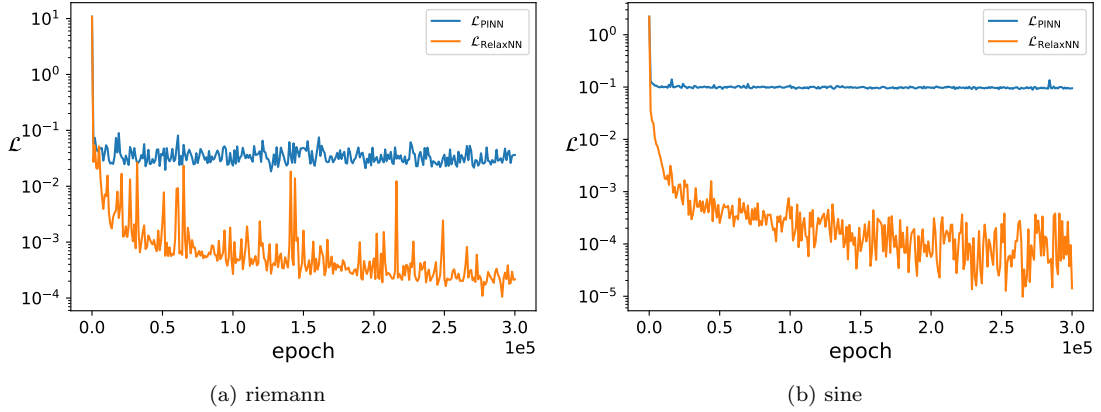


Figure 5: *Burgers' equation*: Comparison of the loss curves of RelaxNN against the one of PINN during the training process: (a) Riemann initial condition. (b) Sine initial condition.

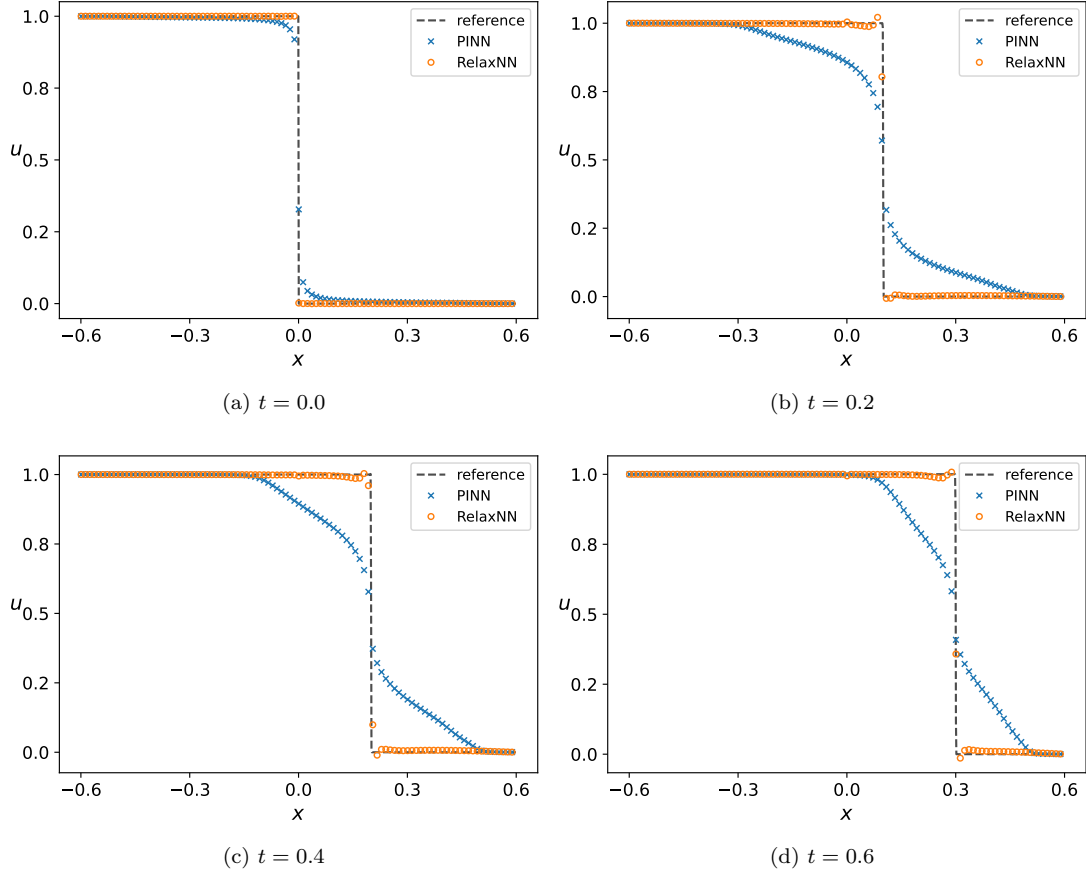


Figure 6: *Burgers' equation with Riemann initial condition*: Comparison among the final epoch prediction of RelaxNN, PINN, and the reference solution spatially at different specific moments. The resulting relative L^2 error of PINN, RelaxNN are 1.64×10^{-2} , 8.29×10^{-4} . For RelaxNN, the configuration of $\mathbf{u}_{\theta_1}^{\text{NN}}$, $\mathbf{v}_{\theta_2}^{\text{NN}}$ are $[2, 128, 128, 128, 128, 1]$ and $[2, 64, 64, 64, 64, 1]$. We training for 300,000 epochs and one step per epoch. Loss weights settings are shown in Table 2. For PINN, all settings are the same as RelaxNN without the extra neural network.

6.1.2 Sine problem

We consider the inviscid Burgers' equation in domain $\Omega = \{(t, x)\} = [0.0, 1.0] \times [-1.0, 1.0]$ with sine initial condition as

$$u_0(0, x) = -\sin(\pi x), \quad -1 \leq x \leq 1. \quad (43)$$

Networks' configurations are presented in Table 1 and weights settings are shown in Table 2. With these settings, we train RelaxNN for 300,000 epochs and one step for every epoch. For the PINN framework, settings are the same without the extra neural network $\mathbf{v}_\beta^{\text{NN}}$. In Figure 5b, We compare the total loss between the PINN and RelaxNN. In Figure 7, we compare the prediction of RelaxNN and PINN at the final epoch for some specific times.

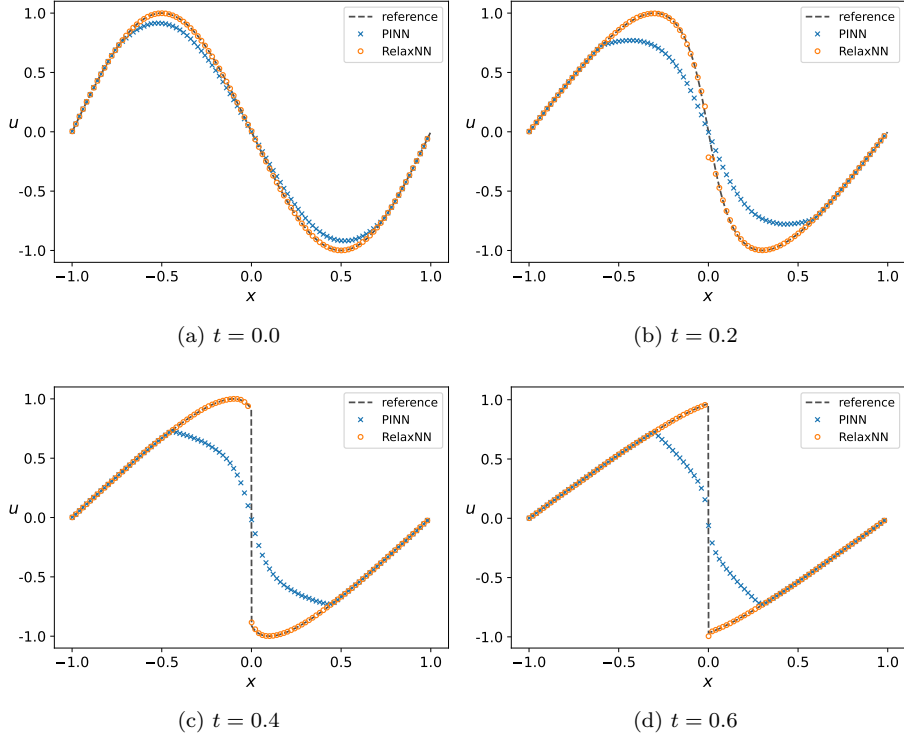


Figure 7: *Burgers' equation with Sine initial condition*: Comparison among the final epoch prediction of RelaxNN, PINN, and the reference solution spatially at different specific moments. The resulting relative L^2 error of PINN, RelaxNN are $1.01 \times 10^{-1}, 3.63 \times 10^{-4}$. For RelaxNN, the configuration of $\mathbf{u}_{\theta_1}^{\text{NN}}, \mathbf{v}_{\theta_2}^{\text{NN}}$ are $[2, 128, 128, 128, 128, 1]$ and $[2, 64, 64, 64, 64, 1]$. We training for 300,000 epochs and one step per epoch. Loss weights settings are shown in Table 2. For PINN, all settings are the same as RelaxNN without the extra neural network.

Problems	Relax level	ω_{residual}		ω_{flux}		ω_{IC}	ω_{BC}
		ω_r^m	ω_r^p	ω_f^m	ω_f^p		
Dam break	type1	0.01	0.01	1.0	1.0	1.0	1.0
Dam break	type2	0.01	0.01		1.0	1.0	1.0
Two shock	type1	0.1	0.1	1.0	1.0	1.0	1.0
Two shock	type2	0.1	0.1		1.0	1.0	1.0

Table 3: *Shallow water equations*: Loss weights settings

6.2 Shallow water equations

6.2.1 Dam break problem

We consider the shallow water equations in domain $\Omega = \{(t, x)\} = [0.0, 1.0] \times [-1.5, 1.5]$ with dam break initial condition as

$$\mathbf{u}_0(0, x) = \begin{pmatrix} 1.0 \\ 0.0 \end{pmatrix}, \quad \text{if } -1.5 \leq x \leq 0.0; \quad \mathbf{u}_0(0, x) = \begin{pmatrix} 0.5 \\ 0.0 \end{pmatrix}, \quad \text{if } 0.0 < x \leq 1.5; \quad (44)$$

Networks' configurations are presented in Table 1 and weights settings are shown in Table 3. With these settings, we train RelaxNN for 600,000 epochs and one step for every epoch. For the PINN framework, settings are the same without the extra neural network $\mathbf{v}_{\theta_2}^{\text{NN}}$. In Figure 8a, We compare the total loss between the PINN and RelaxNN. In Figure 9, we compare the prediction of type1 RelaxNN and PINN at the final epoch for some specific times. Also for type2 RelaxNN in Figure 10.

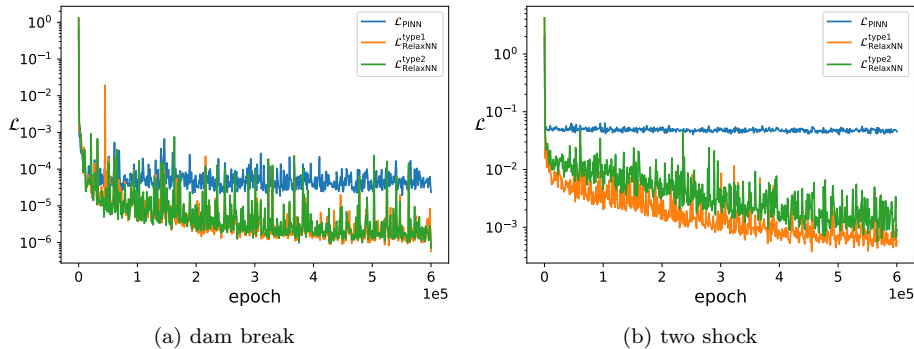


Figure 8: *Shallow water equations*: Comparison of the loss curves of RelaxNN against the one of PINN during the training process. (a)Dam break initial condition. (b)Two shock initial condition.

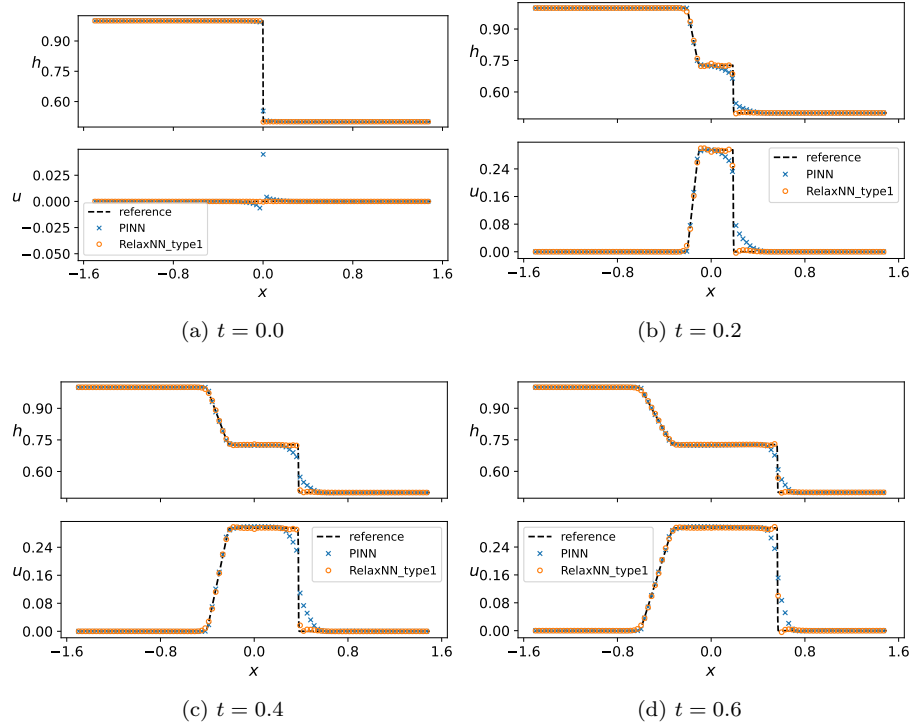


Figure 9: *Shallow water equations with dam break initial condition*: Comparison among the final epoch prediction of RelaxNN(type1), PINN, and the reference solution spatially at different specific moments. The resulting relative L^2 error of PINN, RelaxNN are 4.85×10^{-4} , 9.01×10^{-5} . For RelaxNN, the configuration of $\mathbf{u}_{\theta_1}^{\text{NN}}$, $\mathbf{v}_{\theta_2}^{\text{NN}}$ are $[2,128,128,128,128,128,2]$ and $[2,128,128,128,128,128,2]$. We training for 600,000 epochs and one step per epoch. Loss weights settings are shown in Table 3. For PINN, all settings are the same as RelaxNN without the extra neural network.

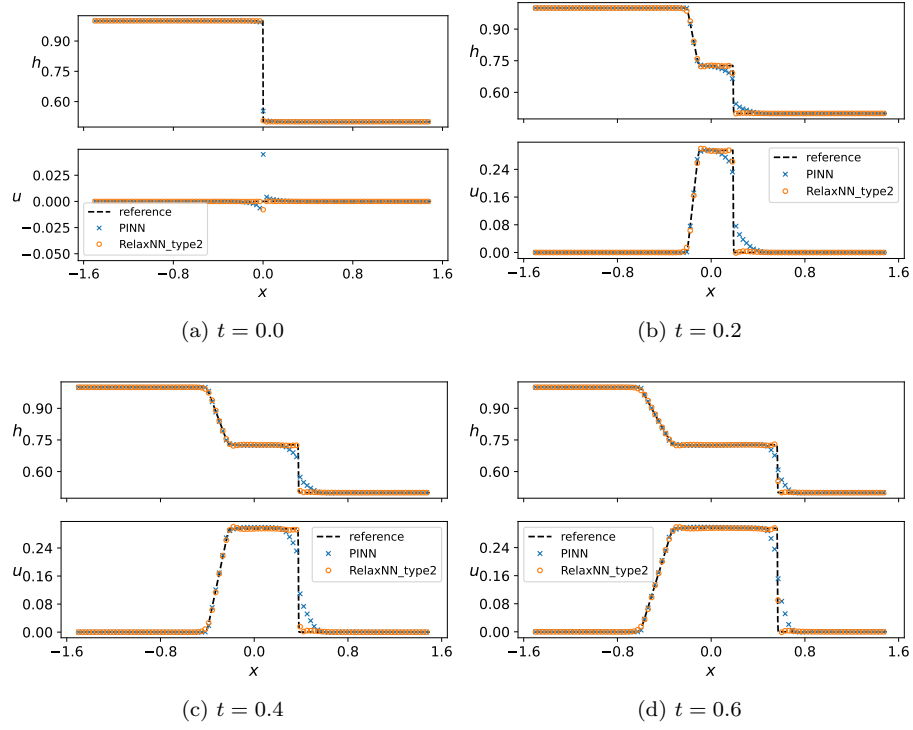


Figure 10: *Shallow water equations with dam break initial condition*: Comparison among the final epoch prediction of RelaxNN(type2), PINN, and the reference solution spatially at different specific moments. The resulting relative L^2 error of PINN, RelaxNN are 4.85×10^{-4} , 7.28×10^{-5} . For RelaxNN, the configuration of $\mathbf{u}_{\theta_1}^{\text{NN}}$, $\mathbf{v}_{\theta_2}^{\text{NN}}$ are $[2,128,128,128,128,2]$ and $[2,64,64,64,64,1]$. We training for 600,000 epochs and one step per epoch. Loss weights settings are shown in Table 3. For PINN, all settings are the same as RelaxNN without the extra neural network.

6.2.2 Two shock problem

We consider the shallow water equations in domain $\Omega = \{(t, x)\} = [0.0, 1.0] \times [-1.0, 1.0]$ with two shock initial condition as

$$\mathbf{u}_0(0, x) = \begin{pmatrix} 1.0 \\ 1.0 \end{pmatrix}, \quad \text{if } -1.0 \leq x \leq 0.0; \quad \mathbf{u}_0(0, x) = \begin{pmatrix} 1.0 \\ -1.0 \end{pmatrix}, \quad \text{if } 0.0 < x \leq 1.0; \quad (45)$$

Networks' configurations are presented in Table 1 and weights settings are shown in Table 3. With these settings, we train RelaxNN for 600,000 epochs and one step for every epoch. For the PINN framework, settings are the same without the extra neural network $\mathbf{v}_{\theta_2}^{\text{NN}}$. In Figure 8b, We compare the total loss between the PINN and RelaxNN. In Figure 11, we compare the prediction of type1 RelaxNN and PINN at the final epoch for some specific times. Also for type2 RelaxNN in Figure 12.

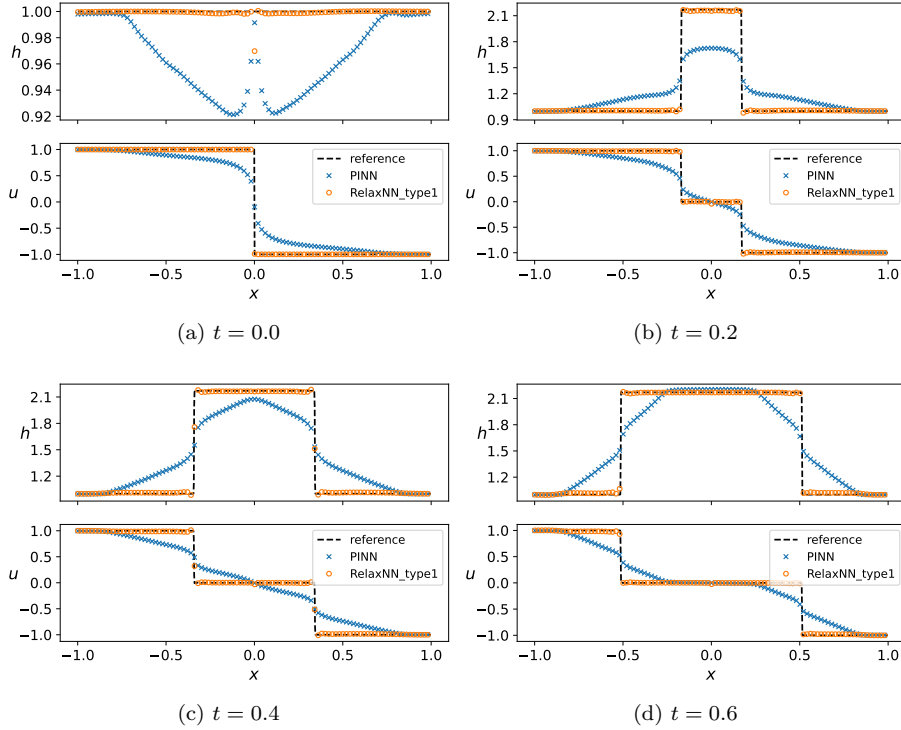


Figure 11: *Shallow water equations with two shock initial condition*: Comparison among the final epoch prediction of RelaxNN(type1), PINN and the reference solution spatially at different specific moments. The resulting relative L^2 error of PINN, RelaxNN are 2.12×10^{-2} , 5.86×10^{-4} . For RelaxNN, the configuration of $\mathbf{u}_{\theta_1}^{\text{NN}}$, $\mathbf{v}_{\theta_2}^{\text{NN}}$ are $[2,128,128,128,128,128,2]$ and $[2,128,128,128,128,128,2]$. We training for 600,000 epochs and one step per epoch. Loss weights settings are shown in Table 3. For PINN, all settings are the same as RelaxNN without the extra neural network.

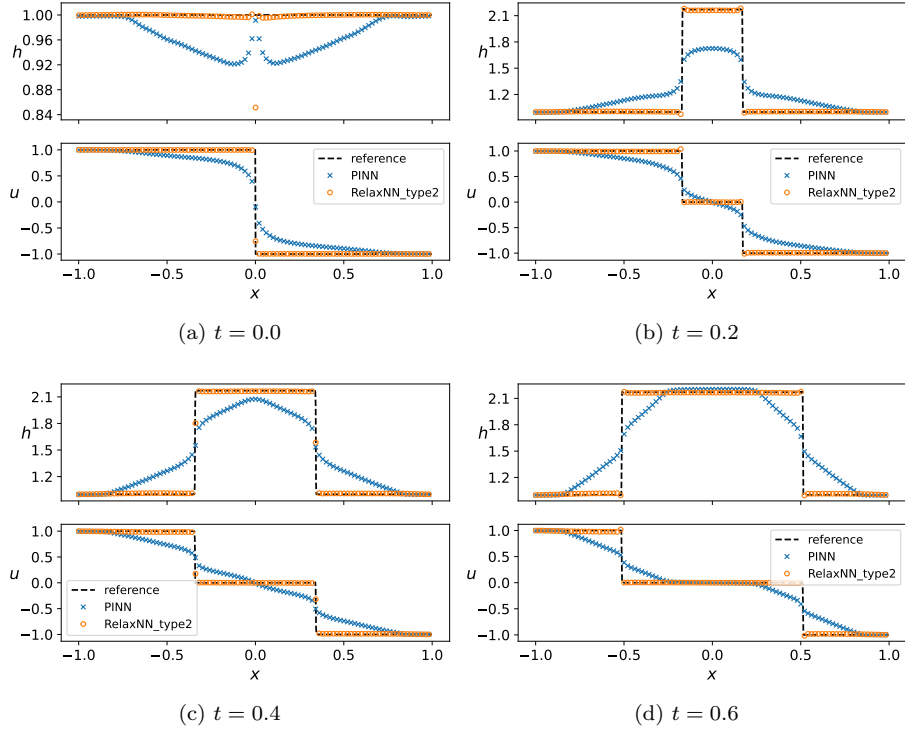


Figure 12: *Shallow water equations with two shock initial condition*: Comparison among the final epoch prediction of RelaxNN(type2), PINN, and the reference solution spatially at different specific moments. The resulting relative L^2 error of PINN, RelaxNN are 2.12×10^{-2} , 2.53×10^{-4} . For RelaxNN, the configuration of $\mathbf{u}_{\theta_1}^{\text{NN}}$, $\mathbf{v}_{\theta_2}^{\text{NN}}$ are $[2, 128, 128, 128, 128, 2]$ and $[2, 64, 64, 64, 64, 1]$. We training for 600,000 epochs and one step per epoch. Loss weights settings are shown in Table 3. For PINN, all settings are the same as RelaxNN without the extra neural network.

Problems	Relax level	ω_{residual}			ω_{flux}			ω_{IC}	ω_{BC}
		ω_r^m	ω_r^p	ω_r^e	ω_f^m	ω_f^p	ω_f^e		
Sod	type1	0.1	0.05	0.01	5.0	5.0	5.0	5.0	5.0
Sod	type2	0.1	0.05	0.01		5.0	5.0	5.0	5.0
Sod	type3	0.1	0.05	0.01			5.0	5.0	5.0
Lax	type1	1.0	0.5	0.1	100.0	100.0	10.0	100.0	100.0
Lax	type2	1.0	0.5	0.1		100.0	10.0	100.0	100.0
Lax	type3	1.0	0.5	0.1			10.0	100.0	100.0

Table 4: *Euler equations*: Loss weights settings.

6.3 Euler equations

6.3.1 Sod problem

We consider the euler equations in domain $\Omega = \{(t, x)\} = [0.0, 0.4] \times [-0.8, 0.8]$ with sod shocktube initial condition as

$$\mathbf{u}_0(0, x) = \begin{pmatrix} 1.0 \\ 0.0 \\ 1.0 \end{pmatrix}, \quad \text{if } x \leq 0.0; \quad \mathbf{u}_0(0, x) = \begin{pmatrix} 0.125 \\ 0.0 \\ 0.1 \end{pmatrix}, \quad \text{if } x > 0.0; \quad (46)$$

Networks' configurations are presented in Table 1 and weights settings are shown in Table 4. With these settings, we train RelaxNN for 600,000 epochs and one step for every epoch. For the PINN framework, settings are the same without the extra neural network $\mathbf{v}_{\theta_2}^{\text{NN}}$. In Figure 13a, We compare the total loss between the PINN and RelaxNN. In Figure 9, we compare the prediction of type1 RelaxNN and PINN at the final epoch for some specific times. Also for type2 RelaxNN in Figure 10.

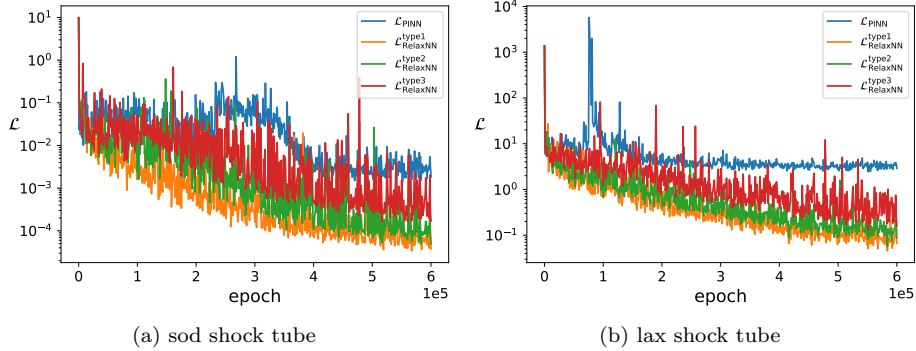


Figure 13: loss curves during the training process of Euler equations

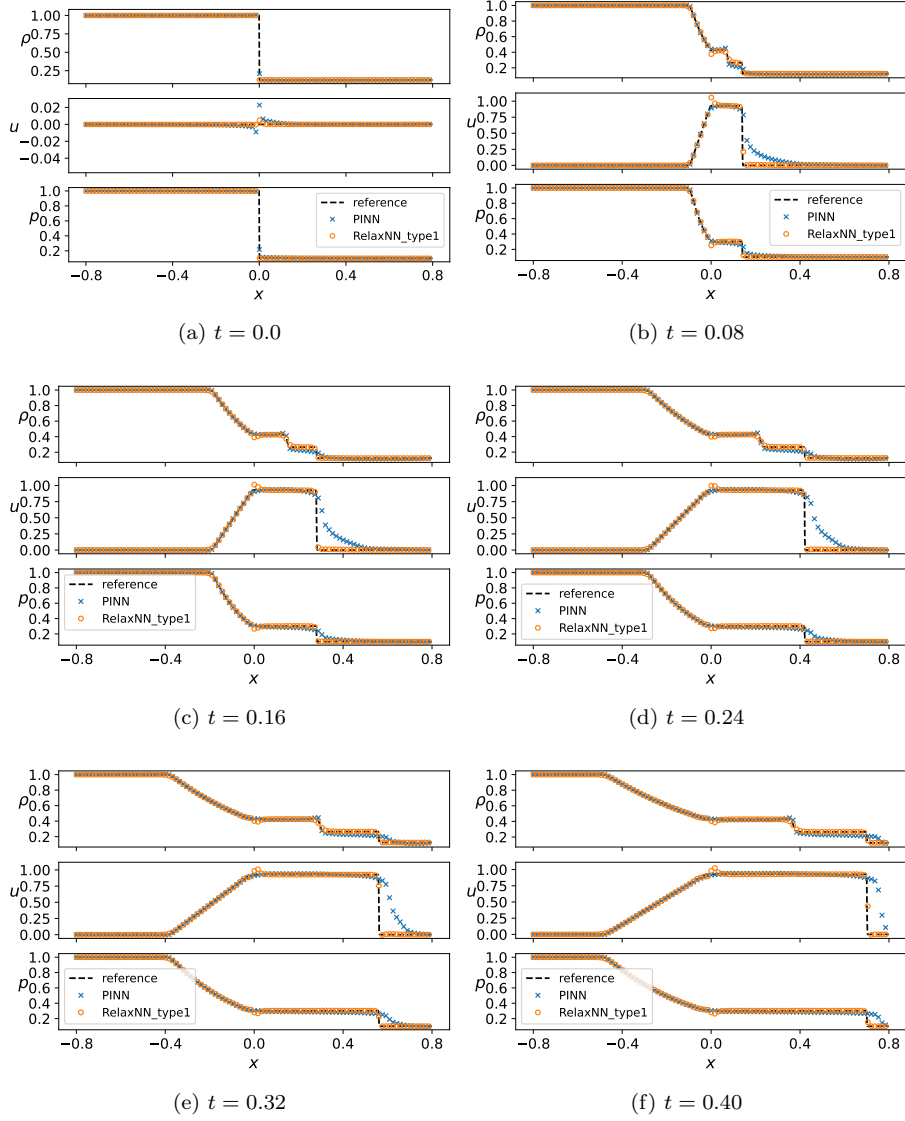


Figure 14: *Euler equations with sod shock tube initial condition*: Comparison among the final epoch prediction of RelaxNN(type1), PINN, and the reference solution spatially at different specific moments. The resulting relative L^2 error of PINN, RelaxNN are 1.43×10^{-2} , 7.61×10^{-4} . For RelaxNN, the configuration of $\mathbf{u}_{\theta_1}^{\text{NN}}$, $\mathbf{v}_{\theta_2}^{\text{NN}}$ are $[2,384,384,384,384,384,3]$ and $[2,384,384,384,384,384,3]$. We training for 600,000 epochs and one step per epoch. Loss weights settings are shown in Table 4. For PINN, all settings are the same as RelaxNN without the extra neural network.

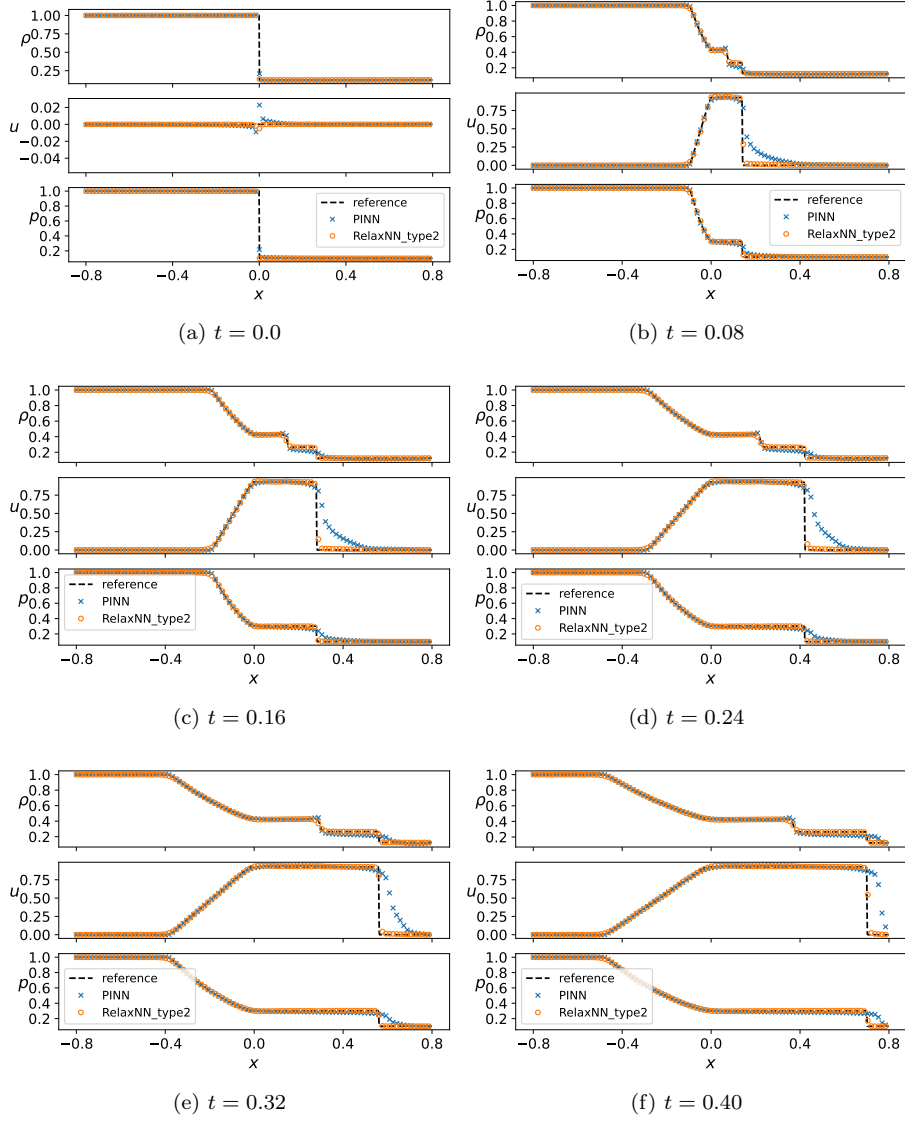


Figure 15: *Euler equations with sod shock tube initial condition*: Comparison among the final epoch prediction of RelaxNN(type2), PINN, and the reference solution spatially at different specific moments. The resulting relative L^2 error of PINN, RelaxNN are 1.43×10^{-2} , 9.76×10^{-4} . For RelaxNN, the configuration of $\mathbf{u}_{\theta_1}^{\text{NN}}$, $\mathbf{v}_{\theta_2}^{\text{NN}}$ are $[2,384,384,384,384,384,3]$ and $[2,256,256,256,256,256,2]$. We training for 600,000 epochs and one step per epoch. Loss weights settings are shown in Table 4. For PINN, all settings are the same as RelaxNN without the extra neural network.

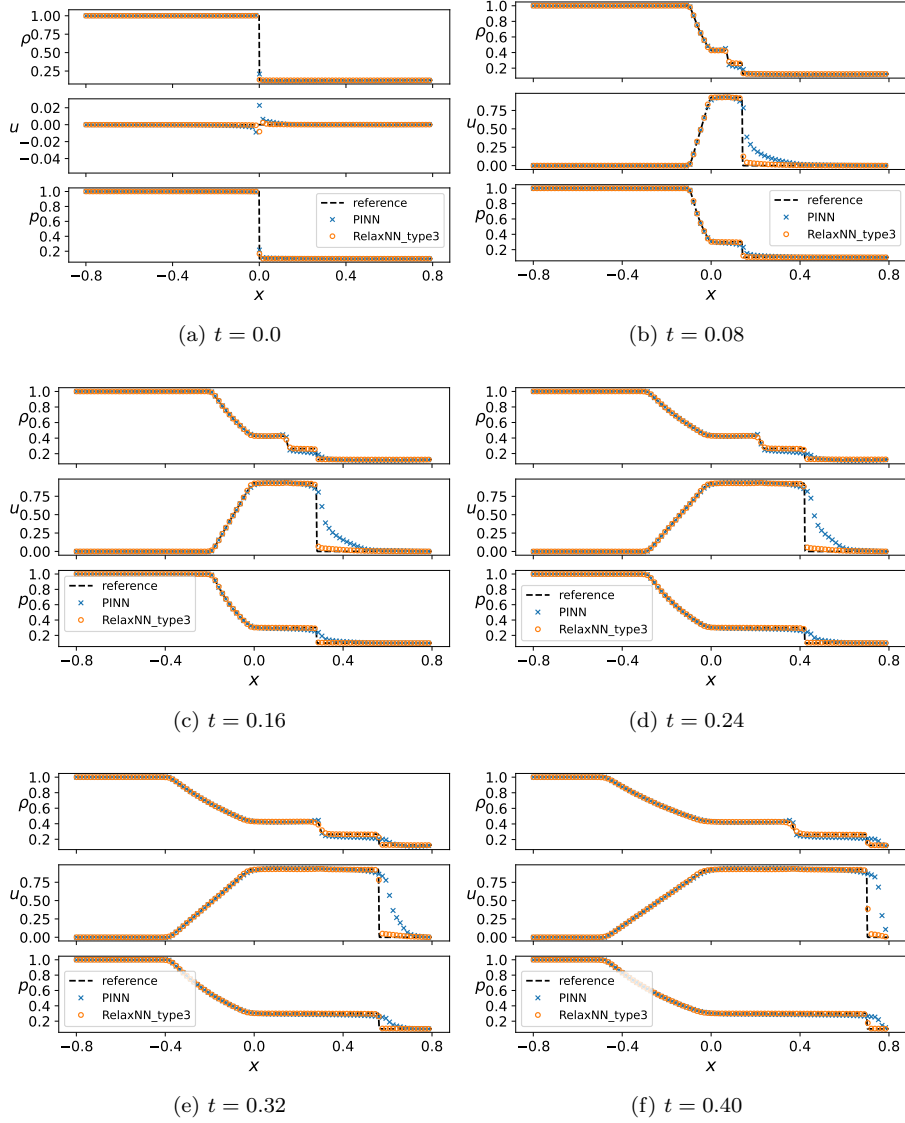


Figure 16: *Euler equations with sod shock tube initial condition*: Comparison among the final epoch prediction of RelaxNN(type3), PINN, and the reference solution spatially at different specific moments. The resulting relative L^2 error of PINN, RelaxNN are 1.43×10^{-2} , 5.91×10^{-4} . For RelaxNN, the configuration of $\mathbf{u}_{\theta_1}^{\text{NN}}$, $\mathbf{v}_{\theta_2}^{\text{NN}}$ are $[2, 384, 384, 384, 384, 384, 3]$ and $[2, 128, 128, 128, 128, 128, 1]$. We training for 600,000 epochs and one step per epoch. Loss weights settings are shown in Table 4. For PINN, all settings are the same as RelaxNN without the extra neural network.

6.3.2 Lax problem

We consider the euler equations in domain $\Omega = \{(t, x)\} = [0.0, 0.16] \times [-0.5, 0.5]$ with lax shocktube initial condition as

$$\mathbf{u}_0(0, x) = \begin{pmatrix} 0.445 \\ 0.698 \\ 3.528 \end{pmatrix}, \quad \text{if } -0.5 \leq x \leq 0.0; \quad \mathbf{u}_0(0, x) = \begin{pmatrix} 0.5 \\ 0.0 \\ 0.571 \end{pmatrix}, \quad \text{if } 0.0 < x \leq 0.5; \quad (47)$$

Networks' configurations are presented in Table 1 and weights settings are shown in Table 4. With these settings, we train RelaxNN for 600,000 epochs and one step for every epoch. For the PINN framework, settings are the same without the extra neural network $\mathbf{v}_{\theta_2}^{\text{NN}}$. In Figure 13b, We compare the total loss between the PINN and RelaxNN. In Figure 17, we compare the prediction of type1 RelaxNN and PINN at the final epoch for some specific times. Also for type2 RelaxNN in Figure 18 and type3 RelaxNN in Figure 19.

6.4 Uncertainty quantification problems

In this part, we consider stochastic perturbation on the initial condition for the equations we discussed above, well known as uncertainty quantification problems. For simplicity, we do not write down the loss term or the loss weights again. All we need is to incorporate the random variables into the inputs of our neural networks. The outstanding performances reveal the potential of our method to solve the high-dimensional problems.

6.4.1 UQ problems in inviscid Burgers' equation with Riemann initial condition

We consider the inviscid Burgers' equation (14) in domain $\Omega = \{(t, x)\} = [0.0, 1.0] \times [-0.6, 0.6]$ with stochastic Riemann initial condition as

$$u_0(0, x, \mathbf{z}) = \begin{cases} 1.0 + \varepsilon \sum_{i=1}^s z_i, & -0.6 \leq x \leq 0 \\ 0.0, & 0 < x \leq 0.6 \end{cases}, \quad (48)$$

where $\mathbf{z} = (z_1, z_2, \dots, z_s) \sim \mathcal{U}([-1, 1]^s)$, $\varepsilon = 0.005$, $s = 100$. We then obtain the reference variance of the solution by the Monte Carlo method for 100,000 random experiments. The mean and variance of the solution of our RelaxNN are also obtained by the Monte Carlo method for 1,000,000 random experiments. Our results are shown in Figure 20.

6.4.2 UQ problems in shallow water equations with two shocks initial condition

We consider the shallow water equations (17) in domain $\Omega = \{(t, x)\} = [0.0, 1.0] \times [-1.0, 1.0]$ with stochastic two shock initial conditions as

$$\mathbf{u}_0(0, x) = \begin{pmatrix} 1.0 \\ 1.0 \end{pmatrix}, \quad \text{if } -1.0 \leq x \leq \psi(\mathbf{z}); \quad \mathbf{u}_0(0, x) = \begin{pmatrix} 1.0 \\ -1.0 \end{pmatrix}, \quad \text{if } \psi(\mathbf{z}) < x \leq 1.0; \quad (49)$$

Where $\psi(\mathbf{z}) = \varepsilon(z_1\sigma(z_2z_3+z_4)+z_5)$, $\sigma(\cdot)$ is the ReLU function and $\varepsilon = 0.005$. We obtain the reference mean and variance of the solution by the Monte Carlo method for 100,000 random experiments. The mean and variance of the solution of our RelaxNN are obtained by numerical quadrature. Specifically, we used the Gaussian-legendre quadrature with 10 points in every dimension. In Figure 21, we display our results.

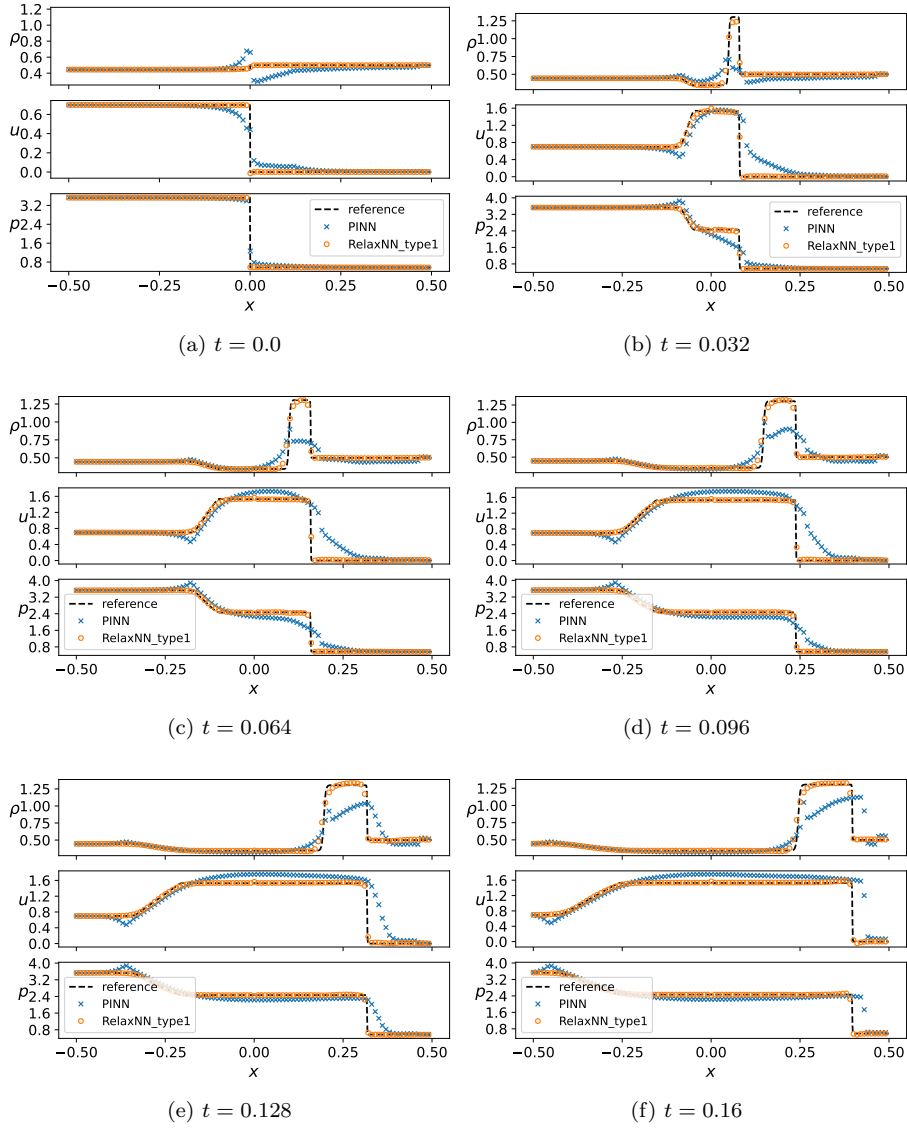


Figure 17: *Euler equations with lax shock tube initial condition*: Comparison among the final epoch prediction of RelaxNN(type1), PINN, and the reference solution spatially at different specific moments. The resulting relative L^2 error of PINN, RelaxNN are 1.99×10^{-2} , 6.94×10^{-4} . For RelaxNN, the configuration of $\mathbf{u}_{\theta_1}^{\text{NN}}$, $\mathbf{v}_{\theta_2}^{\text{NN}}$ are $[2,384,384,384,384,384,3]$ and $[2,384,384,384,384,384,3]$. We training for 600,000 epochs and one step per epoch. Loss weights settings are shown in Table 4. For PINN, all settings are the same as RelaxNN without the extra neural network.

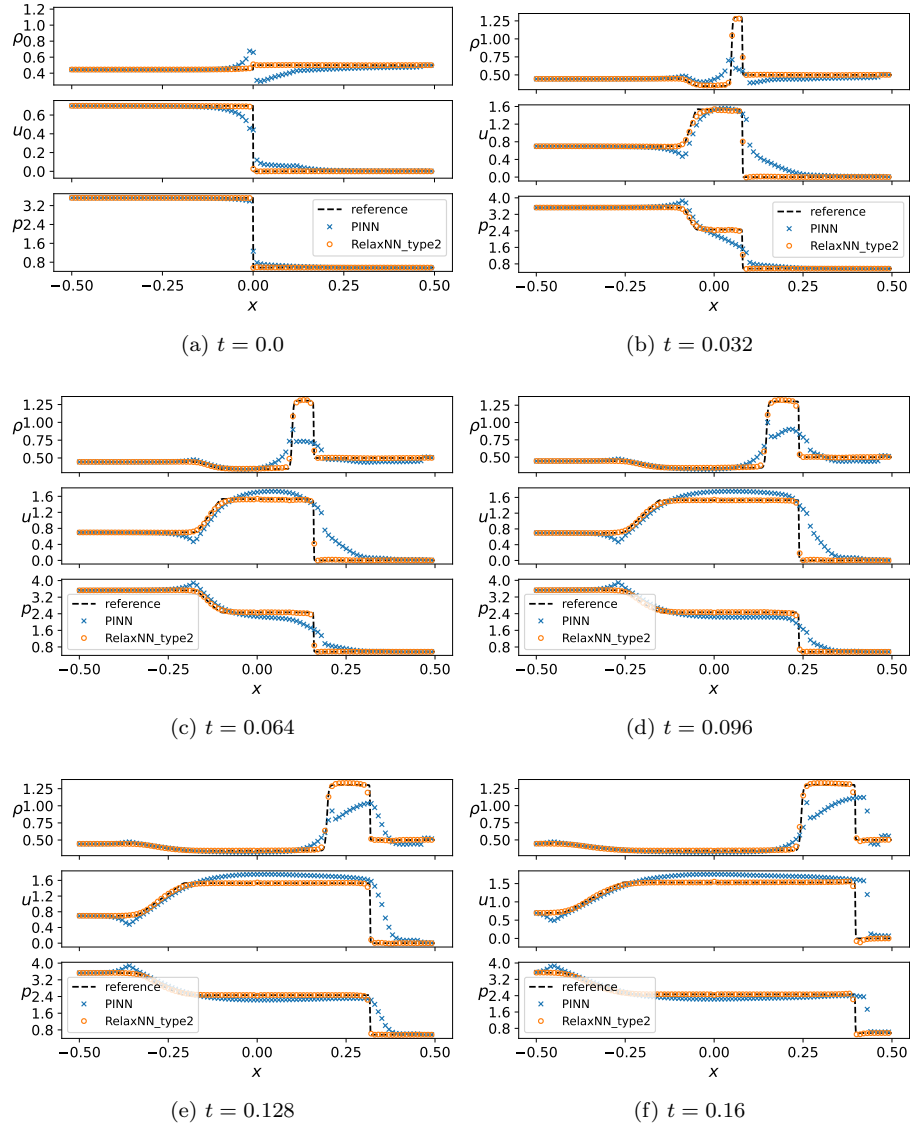


Figure 18: *Euler equations with lax shock tube initial condition*: Comparison among the final epoch prediction of RelaxNN(type1), PINN, and the reference solution spatially at different specific moments. The resulting relative L^2 error of PINN, RelaxNN are 1.99×10^{-2} , 7.34×10^{-4} . For RelaxNN, the configuration of $\mathbf{u}_{\theta_1}^{\text{NN}}$, $\mathbf{v}_{\theta_2}^{\text{NN}}$ are $[2,384,384,384,384,384,3]$ and $[2,256,256,256,256,256,2]$. We training for 600,000 epochs and one step per epoch. Loss weights settings are shown in Table 4. For PINN, all settings are the same as RelaxNN without the extra neural network.

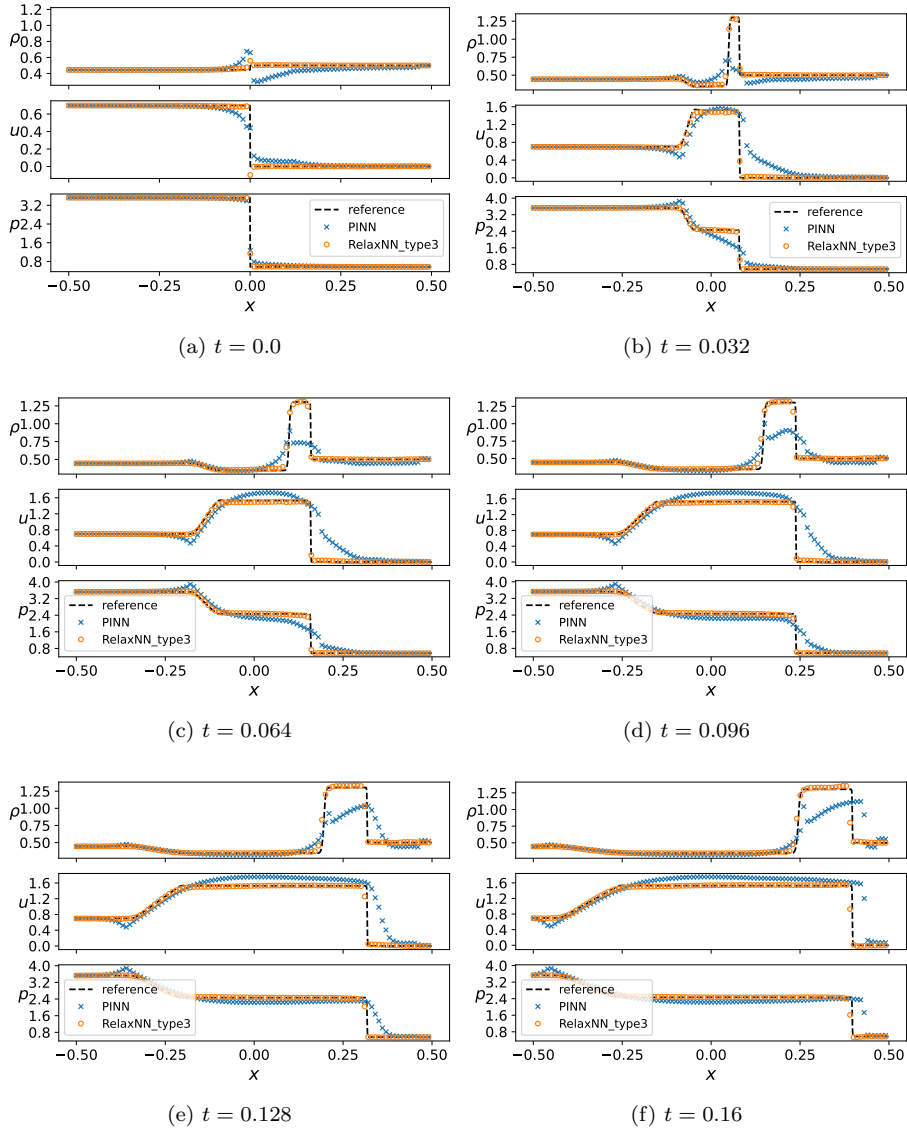


Figure 19: *Euler equations with lax shock tube initial condition*: Comparison among the final epoch prediction of RelaxNN(type1), PINN, and the reference solution spatially at different specific moments. The resulting relative L^2 error of PINN, RelaxNN are 1.99×10^{-2} , 1.68×10^{-3} . For RelaxNN, the configuration of $\mathbf{u}_{\theta_1}^{\text{NN}}$, $\mathbf{v}_{\theta_2}^{\text{NN}}$ are $[2,384,384,384,384,384,3]$ and $[2,128,128,128,128,128,1]$. We training for 600,000 epochs and one step per epoch. Loss weights settings are shown in Table 4. For PINN, all settings are the same as RelaxNN without the extra neural network.

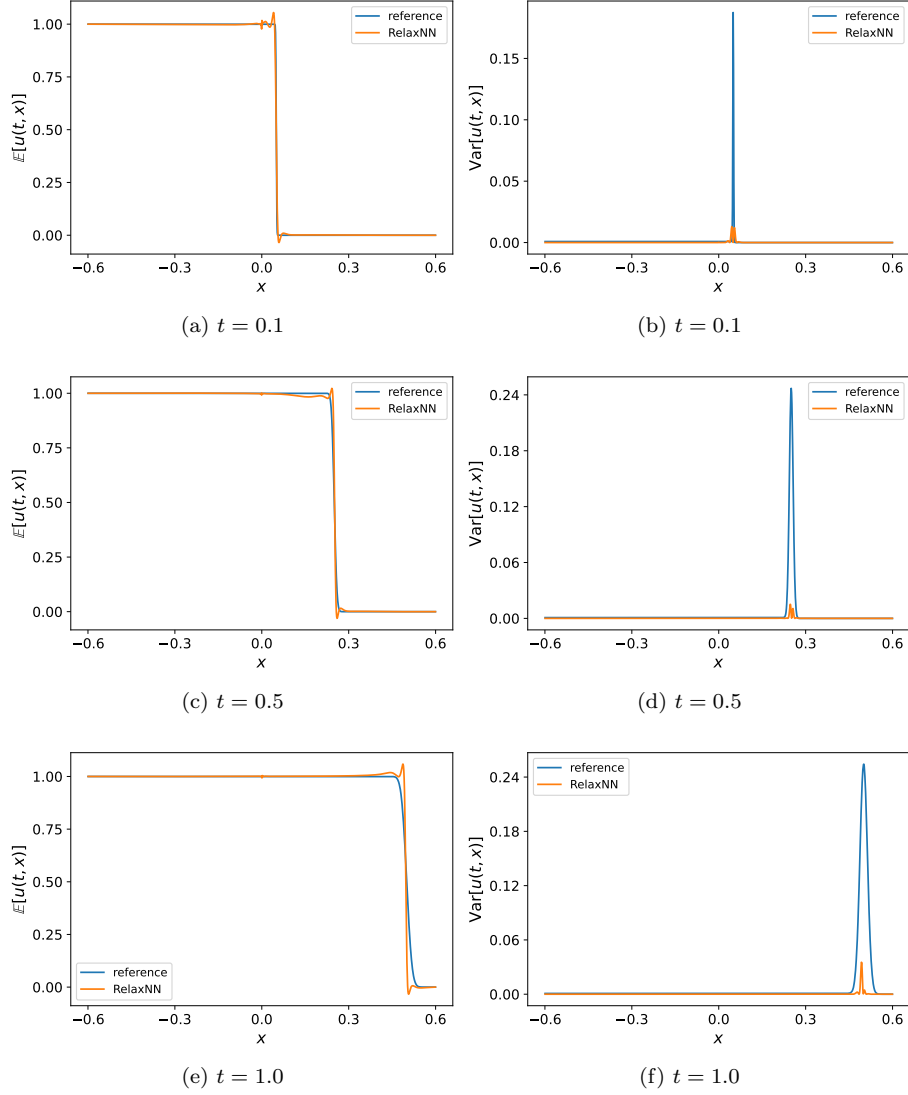


Figure 20: *Burgers' equation with stochastic Riemann initial condition*: Comparison among the final epoch prediction of RelaxNN(type3), and the reference solution spatially at different specific moments. The relative L^2 error of expectation, variance are 2.40×10^{-2} , 3.42×10^{-2} . For RelaxNN, the configuration of $\mathbf{u}_{\theta_1}^{\text{NN}}$, $\mathbf{v}_{\theta_2}^{\text{NN}}$ are $[102, 128, 128, 128, 1]$ and $[102, 64, 64, 64, 1]$. We training for 300,000 epochs and one step per epoch.

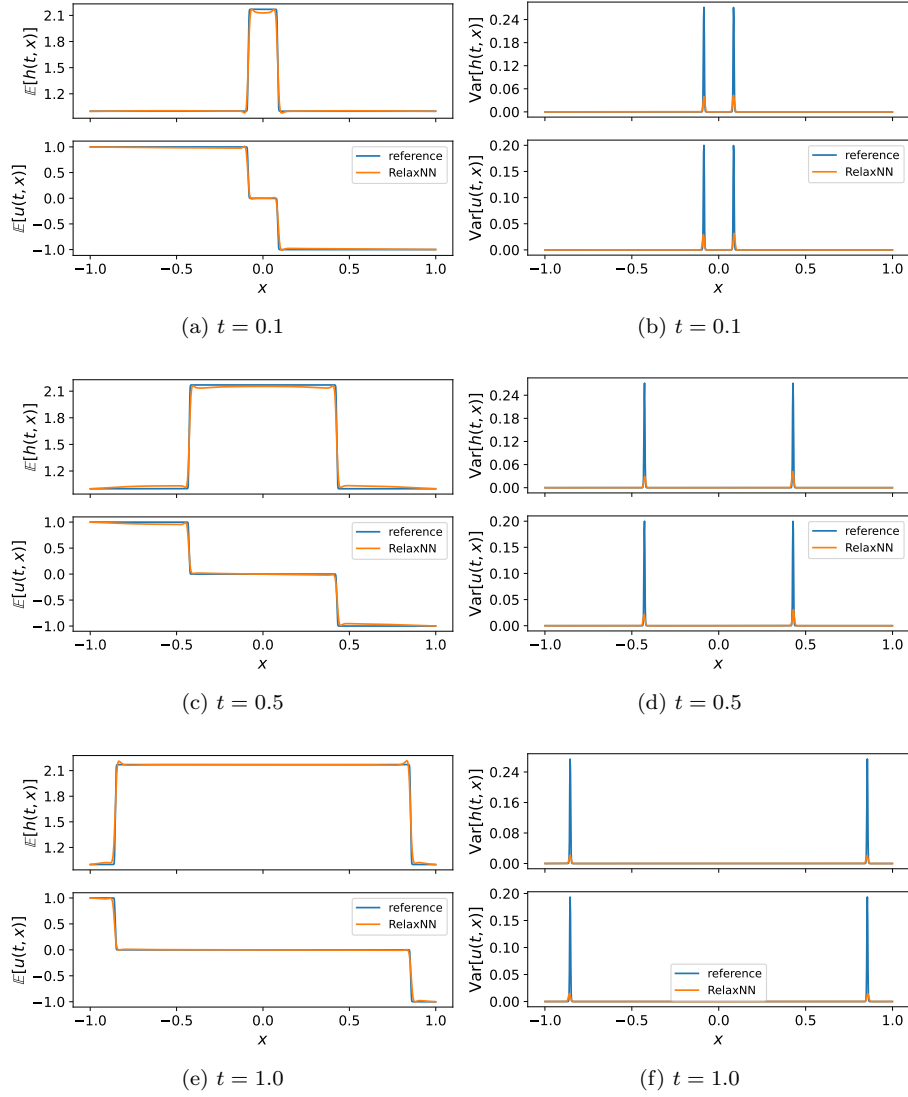


Figure 21: *Shallow water equations with stochastic two shock initial conditions*: Comparison among the final epoch prediction of RelaxNN(type3) and the reference solution spatially at different specific moments. The resulting relative L^2 error of mean and variance are 2.24×10^{-2} , 2.60×10^{-2} . For RelaxNN, the configuration of $\mathbf{u}_{\theta_1}^{\text{NN}}$, $\mathbf{v}_{\theta_2}^{\text{NN}}$ are $[7, 256, 256, 256, 256, 256, 2]$ and $[7, 128, 128, 128, 128, 128, 1]$. We training for 600,000 epochs and one step per epoch. Loss weights settings are shown in Table 4.

6.4.3 UQ problems in Euler equations with Sod initial condition

We consider the Euler equations (26) in domain $\Omega = \{(t, x)\} = [0.0, 0.4] \times [-0.8, 0.8]$ with stochastic Sod shock tube initial condition as

$$\mathbf{u}_0(0, x) = \begin{pmatrix} 1.0 \\ 0.0 \\ 1.0 \end{pmatrix}, \quad \text{if } -0.8 \leq x \leq \psi(\mathbf{z}); \quad \mathbf{u}_0(0, x) = \begin{pmatrix} 0.125 \\ 0.0 \\ 0.1 \end{pmatrix}, \quad \text{if } \psi(\mathbf{z}) \leq x \leq 0.8; \quad (50)$$

Where $\psi(\mathbf{z}) = \varepsilon(z_1\sigma(z_2z_3+z_4)+z_5)$, $\sigma(\cdot)$ is the ReLU function and $\varepsilon = 0.005$. We obtain the reference mean and variance of the solution by the Monte Carlo method for 100,000 random experiments. The mean and variance of the solution of our RelaxNN are obtained by numerical quadrature. Also, we used the Gaussian-legendre quadrature with 10 points in every dimension. In Figure 22, we display our results.

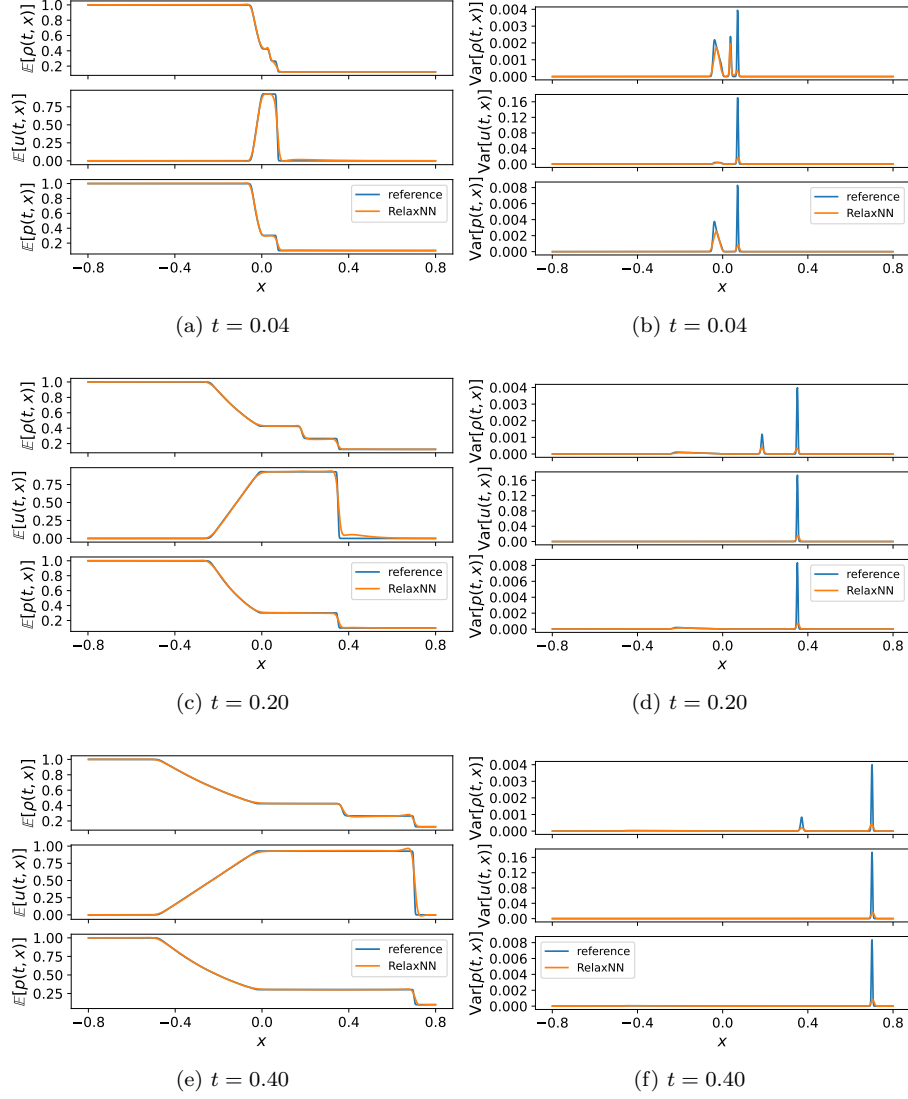


Figure 22: *Euler equations with stochastic Sod shock tube initial condition*: Comparison among the final epoch prediction of RelaxNN(type3) and the reference solution spatially at different specific moments. The resulting relative L^2 error of mean and variance are 2.26×10^{-2} , 1.71×10^{-2} . For RelaxNN, the configuration of $\mathbf{u}_{\theta_1}^{\text{NN}}$, $\mathbf{v}_{\theta_2}^{\text{NN}}$ are $[7, 384, 384, 384, 384, 384, 3]$ and $[7, 128, 128, 128, 128, 128, 1]$. We training for 600,000 epochs and one step per epoch. Loss weights settings are shown in Table 4.

References

- [1] Sergueï Konstantinovitch Godunov. A difference method for numerical calculation of discontinuous equations of hydrodynamics. *Math. Sb*, 47:217, 1959.
- [2] Ami Harten, Bjorn Engquist, Stanley Osher, and Sukumar R Chakravarthy. *Uniformly high order accurate essentially non-oscillatory schemes, III*. Springer, 1997.
- [3] Guang-Shan Jiang and Chi-Wang Shu. Efficient implementation of weighted eno schemes. *Journal of computational physics*, 126(1):202–228, 1996.
- [4] Bernardo Cockburn, George Karniadakis, and Shu (Eds. *Discontinuous Galerkin Methods: Theory, Computation and Application*, volume 11. Springer Science & Business Media, 12 2000. ISBN 978-3-642-64098-8. doi: 10.1007/978-3-642-59721-3.
- [5] John VonNeumann and Robert D Richtmyer. A method for the numerical calculation of hydrodynamic shocks. *Journal of applied physics*, 21(3):232–237, 1950.
- [6] Shi Jin. Asymptotic preserving (ap) schemes for multiscale kinetic and hyperbolic equations: a review. *Lecture notes for summer school on methods and models of kinetic theory (M&MKT), Porto Ercole (Grosseto, Italy)*, pages 177–216, 2010.
- [7] MWMG Dissanayake and Nhan Phan-Thien. Neural-network-based approximations for solving partial differential equations. *communications in Numerical Methods in Engineering*, 10(3): 195–201, 1994.
- [8] Kurt Hornik, Maxwell Stinchcombe, and Halbert White. Multilayer feedforward networks are universal approximators. *Neural networks*, 2(5):359–366, 1989.
- [9] Maziar Raissi, Paris Perdikaris, and George E Karniadakis. Physics-informed neural networks: A deep learning framework for solving forward and inverse problems involving nonlinear partial differential equations. *Journal of Computational Physics*, 378:686–707, 2019.
- [10] George Em Karniadakis, Ioannis G Kevrekidis, Lu Lu, Paris Perdikaris, Sifan Wang, and Liu Yang. Physics-informed machine learning. *Nature Reviews Physics*, 3(6):422–440, 2021.
- [11] Atilim Gunes Baydin, Barak A Pearlmutter, Alexey Andreyevich Radul, and Jeffrey Mark Siskind. Automatic differentiation in machine learning: a survey. *Journal of Machine Learning Research*, 18:1–43, 2018.
- [12] Aditi Krishnapriyan, Amir Gholami, Shandian Zhe, Robert Kirby, and Michael W Mahoney. Characterizing possible failure modes in physics-informed neural networks. *Advances in Neural Information Processing Systems*, 34:26548–26560, 2021.
- [13] Sifan Wang, Yujun Teng, and Paris Perdikaris. Understanding and mitigating gradient flow pathologies in physics-informed neural networks. *SIAM Journal on Scientific Computing*, 43 (5):A3055–A3081, 2021.
- [14] Arka Daw, Jie Bu, Sifan Wang, Paris Perdikaris, and Anuj Karpatne. Mitigating propagation failures in physics-informed neural networks using retain-resample-release (r3) sampling. *arXiv preprint arXiv:2207.02338*, 2023.

- [15] Aidan Chaumet and Jan Giesselmann. Efficient wpinn-approximations to entropy solutions of hyperbolic conservation laws. *arXiv preprint arXiv:2211.12393*, 2022.
- [16] Archie J Huang and Shaurya Agarwal. On the limitations of physics-informed deep learning: Illustrations using first order hyperbolic conservation law-based traffic flow models. *IEEE Open Journal of Intelligent Transportation Systems*, 2023.
- [17] Ravi G Patel, Indu Manickam, Nathaniel A Trask, Mitchell A Wood, Myoungkyu Lee, Ignacio Tomas, and Eric C Cyr. Thermodynamically consistent physics-informed neural networks for hyperbolic systems. *Journal of Computational Physics*, 449:110754, 2022.
- [18] Tim De Ryck, Siddhartha Mishra, and Roberto Molinaro. Weak physics informed neural networks for approximating entropy solutions of hyperbolic conservation laws. In *Seminar für Angewandte Mathematik, Eidgenössische Technische Hochschule, Zürich, Switzerland, Rep*, volume 35, page 2022, 2022.
- [19] Li Liu, Shengping Liu, Heng Yong, Fansheng Xiong, and Tengchao Yu. Enhancing the shock-capturing ability of physics-informed neural network by weakening its expression near shocks. *Authorea Preprints*, 2023.
- [20] Craig Michoski, Miloš Milosavljević, Todd Oliver, and David R Hatch. Solving differential equations using deep neural networks. *Neurocomputing*, 399:193–212, 2020.
- [21] Pao-Hsiung Chiu, Jian Cheng Wong, Chinchun Ooi, My Ha Dao, and Yew-Soon Ong. Can-pinn: A fast physics-informed neural network based on coupled-automatic-numerical differentiation method. *Computer Methods in Applied Mechanics and Engineering*, 395:114909, 2022. ISSN 0045-7825. doi: <https://doi.org/10.1016/j.cma.2022.114909>. URL <https://www.sciencedirect.com/science/article/pii/S0045782522001906>.
- [22] Shi Jin and Zhouping Xin. The relaxation schemes for systems of conservation laws in arbitrary space dimensions. *Communications on pure and applied mathematics*, 48(3):235–276, 1995.
- [23] Jingwei Hu and Shi Jin. *Uncertainty Quantification for Kinetic Equations*, pages 193–229. Springer International Publishing, Cham, 2017. ISBN 978-3-319-67110-9. doi: 10.1007/978-3-319-67110-9_6. URL https://doi.org/10.1007/978-3-319-67110-9_6.
- [24] Bing Yu et al. The deep ritz method: a deep learning-based numerical algorithm for solving variational problems. *Communications in Mathematics and Statistics*, 6(1):1–12, 2018.
- [25] Dongkun Zhang, Lu Lu, Ling Guo, and George Em Karniadakis. Quantifying total uncertainty in physics-informed neural networks for solving forward and inverse stochastic problems. *Journal of Computational Physics*, 397:108850, 2019.
- [26] E Weinan. Machine learning and computational mathematics. *arXiv preprint arXiv:2009.14596*, 2020.
- [27] Yaohua Zang, Gang Bao, Xiaojing Ye, and Haomin Zhou. Weak adversarial networks for high-dimensional partial differential equations. *Journal of Computational Physics*, 411:109409, 2020.

- [28] E Weinan, Jiequn Han, and Arnulf Jentzen. Algorithms for solving high dimensional pdes: from nonlinear monte carlo to machine learning. *Nonlinearity*, 35(1):278, 2021.
- [29] Jingrun Chen, Shi Jin, and Liyao Lyu. A deep learning based discontinuous galerkin method for hyperbolic equations with discontinuous solutions and random uncertainties. *arXiv preprint arXiv:2107.01127*, 2021.
- [30] Clawpack Development Team. Clawpack software, 2020. URL <http://www.clawpack.org>. Version 5.7.1.
- [31] Randall J. LeVeque. *Finite Volume Methods for Hyperbolic Problems*. Cambridge Texts in Applied Mathematics. Cambridge University Press, 2002. doi: 10.1017/CBO9780511791253.
- [32] Sydney Chapman and Thomas George Cowling. *The mathematical theory of non-uniform gases: an account of the kinetic theory of viscosity, thermal conduction and diffusion in gases*. Cambridge university press, 1990.
- [33] Tai-Ping Liu. Hyperbolic conservation laws with relaxation. *Communications in Mathematical Physics*, 108:153–175, 1987.
- [34] G Chen, C Levermore, and T Liu. Hyperbolic conservation laws with sti relaxation terms and entropy, submitted to comm. *Pure Appl. Math*, 1992.
- [35] Xin Liu, Xi Chen, Shi Jin, Alexander Kurganov, Tong Wu, and Hui Yu. Moving-water equilibria preserving partial relaxation scheme for the saint-venant system. *SIAM Journal on Scientific Computing*, 42(4):A2206–A2229, 2020.
- [36] I Suliciu. On modelling phase transitions by means of rate-type constitutive equations. shock wave structure. *International Journal of Engineering Science*, 28(8):829–841, 1990.
- [37] Ion Suliciu. On the thermodynamics of rate-type fluids and phase transitions. i. rate-type fluids. *International journal of engineering science*, 36(9):921–947, 1998.
- [38] Frédéric Coquel and Benoit Perthame. Relaxation of energy and approximate riemann solvers for general pressure laws in fluid dynamics. *SIAM Journal on Numerical Analysis*, 35(6): 2223–2249, 1998.
- [39] Kaiming He, Xiangyu Zhang, Shaoqing Ren, and Jian Sun. Delving deep into rectifiers: Surpassing human-level performance on imagenet classification. In *Proceedings of the IEEE international conference on computer vision*, pages 1026–1034, 2015.
- [40] Diederik P Kingma and Jimmy Ba. Adam: A method for stochastic optimization. In *ICLR*, 2015.